



(12) **EUROPEAN PATENT SPECIFICATION**

(45) Date of publication and mention
of the grant of the patent:
03.07.2002 Bulletin 2002/27

(21) Application number: **95940361.9**

(22) Date of filing: **07.12.1995**

(51) Int Cl.7: **F04D 29/28**

(86) International application number:
PCT/GB95/02904

(87) International publication number:
WO 97/21035 (12.06.1997 Gazette 1997/25)

(54) **TURBOMACHINERY AND METHOD OF MANUFACTURING THE SAME**

TURBOMASCHINE UND IHR HERSTELLUNGSVERFAHREN

TURBOMACHINES ET LEUR PROCEDE DE FABRICATION

(84) Designated Contracting States:
CH DE DK FR GB IT LI NL SE

(43) Date of publication of application:
23.09.1998 Bulletin 1998/39

(73) Proprietors:
• **EBARA CORPORATION**
Ohta-ku Tokyo 144 (JP)
• **Ebara Research Co., Ltd.**
Fujisawa-shi, Kanagawa-ken 251 (JP)
• **UNIVERSITY COLLEGE LONDON**
London WC1E 7JE (GB)

(72) Inventors:
• **GOTO, Akira**
Fujisawa-shi, Kanagawa-ken 251 (JP)
• **ZANGENEH, Mehrdad**
London N6 5PY (GB)
• **HARADA, Hideomi**
Fujisawa-shi, Kanagawa-ken 251 (JP)

(74) Representative: **Brunner, Michael John**
GILL JENNINGS & EVERY,
Broadgate House,
7 Eldon Street
London EC2M 7LH (GB)

(56) References cited:
WO-A-85/01992 **DE-C- 333 336**
FR-A- 2 550 585 **GB-A- 2 224 083**
US-A- 3 481 531

- **THE AMERICAN SOCIETY OF MECHANICAL ENGINEERS, 1988, NEW YORK, pages 1-7, XP000563980 ZHONGOI, W: "An Experimental Investigation into the Reasons of Reducing Secondary Flow Losses by Using Leaned Blades in Rectangular Turbine Cascades with Incidence Angle" cited in the application**
- **THE AMERICAN SOCIETY OF MECHANICAL ENGINEERS, vol. 112, 1990, NEW YORK, pages 346-354, XP000563997 BORGES, J.E.: "A Three-Dimensional Inverse Method for Turbomachinery:Part 1-Theory" cited in the application**
- **INTERNATIONAL JOURNAL FOR NUMERICAL METHODS IN FLUIDS, vol. 17, no. 12, 30 December 1993, CHICHESTER, pages 1019-1144, XP000563982 BORGES, J.E.: "A proposed through-flow inverse method for the design of mixed-flow pumps " cited in the application**
- **THE AMERICAN SOCIETY OF MECHANICAL ENGINEERS, vol. 115, July 1993, NEW YORK, pages 602-613, XP000564765 YANG, Y. L.: "Aerodynamic Design of Turbomachinery Blading in Three-Dimensional Flow: An Application to Radial Inflow Turbines." cited in the application**
- **INTERNATIONAL JOURNAL OF NUMERICAL METHODS IN FLUIDS, vol. 13, 1991, CHICHESTER, pages 599-624, XP000563989 ZANGENEH, M.: "A Compressible Three-Dimensional Design Method for Radial and Mixed Flow Turbomachinery Blades" cited in the application**

Note: Within nine months from the publication of the mention of the grant of the European patent, any person may give notice to the European Patent Office of opposition to the European patent granted. Notice of opposition shall be filed in a written reasoned statement. It shall not be deemed to have been filed until the opposition fee has been paid. (Art. 99(1) European Patent Convention).

- THE AMERICAN SOCIETY OF MECHANICAL ENGINEERS, vol. 115, 1993, NEW YORK, pages 354-361, XP000563986 DANG, T. Q.: "A Fully Three-Dimensional Inverse Method for Turbomachinery Blading in Transonic Flows" cited in the application

- THE AMERICAN SOCIETY OF MECHANICAL ENGINEERS, vol. 85, no. 3, September 1963, NEW YORK, pages 401-416, XP000560640 SMITH, L. H.: "Sweep and Dihedral Effects in Axial-Flow Turbomachinery" cited in the application

Description**Technical Field**

5 **[0001]** The present invention relates to a turbomachinery and a method of manufacturing the turbomachinery which includes a centrifugal pump or a mixed flow pump for pumping liquid, a blower or a compressor for compression of gas, and more particularly to a turbomachinery having an impeller which has a fluid dynamically improved blade profile for suppressing meridional component of secondary flow, and a method of manufacturing such a turbomachinery.

Background Art

10 **[0002]** Conventionally, in flow channels of an impeller in a centrifugal or a mixed flow turbomachinery, main flow flowing along the flow channels are affected by secondary flow generated by movement of low energy fluid in boundary layers on wall surfaces due to static pressure gradients in the flow channels. This phenomenon leads to the formation of streamwise vortices or flow having non-uniform velocity in the flow channel, which in turn results in a substantial fluid energy loss not only in the impeller but also in the diffuser or guide vanes downstream of the impeller.

15 **[0003]** The secondary flow is defined as flow which has a velocity component perpendicular to the main flow. The total energy loss caused by the secondary flows is referred to as the secondary flow loss. The low energy fluid accumulated at a certain region in the flow channel may cause a flow separation in a large scale, thus producing positively sloped characteristic curve and hence preventing the stable operation of the turbomachine.

20 **[0004]** There is a known approach for suppressing the secondary flows in a turbomachine which is to make the impeller have a specific flow channel geometry. As an example of such approach using a specific flow channel geometry, there is a known method in which blades of the impeller in an axial turbomachine are leaned towards the circumferential direction thereof or the direction of suction or discharge side (L.H.Smith and H.Yeh, "Sweep and Dihedral Effects in Axial Flow Turbomachinery", Trans ASME, Journal of Basic Engineering, Vol.85, No.3, 1963, pp.401-416), or a method in which blades in a turbine cascade are leaned or curved toward a circumferential direction thereof (W.Zhongqi, et al., "An Experimental Investigation into the Reasons of Reducing Secondary Flow Losses by Using Leaned Blades in Rectangular Turbine Cascades with Incidence Angle", ASME Paper 88-GT-4), or a method in which a radial rotor has a blade curvature in the spanwise direction with a convex blade pressure surface and/or a concave blade suction surface (GB2224083A). These methods are known to have a favorable influence upon the secondary flows in the flow channel if applied appropriately.

25 **[0005]** However, since the influence of the profile of a blade camber line or a blade cross-section upon the secondary flow has not been essentially known, the effect of blade lean or spanwise blade curvature is utilized under a certain limitation without changing the blade camber line or the blade cross-section substantially. Further, the Japanese laid-open Patent Publication No. 63-10281 discloses a structure in which a projecting portion is provided at the corner of a hub surface and a blade surface in a turbomachine to reduce the secondary flow loss. Since such flow channel profile is a specific blade profile having a nonaxisymmetric hub surface, it is difficult to manufacture the impeller.

30 **[0006]** In all cases of the above prior arts, the method of achieving the effect universally has not been sufficiently studied. Therefore, the universal methods of suppressing the secondary flows under different design conditions and for the different types of turbomachine have not been established. Under these circumstances, there are many cases that the above effect is reduced, or to make matters worse, undesirable effects are obtained.

35 **[0007]** In general, the three-dimensional geometry of the impeller is defined as a meridional geometry formed by a hub surface and a shroud surface and a blade profile serving to transmit energy to fluid. As the meridional geometry, various geometries including a centrifugal type, a mixed flow type and an axial flow type are selected in accordance with design specification, including flow rate, pressure head and rotational speed, which is required in the individual turbomachinery. As a type number characterizing the meridional geometry of an impeller, a specific speed $N_s = NQ^{1/2}/H^{3/4}$ (for pumps), is widely used for designing of the impeller. Here, N is the rotational speed in revolutions per minutes (rpm), Q is the flow rate in cubic meter per minute (m^3/min) and H is the head in meter (m) representing fluid energy which is imparted to the fluid by the turbomachinery. That is, the specific speed is determined if the design specification is given, and the meridional geometry of the impeller can be suitably selected in accordance with the specific speed. Incidentally, Q is defined as volume flow rate, and in case of a compressor or the like, the volume flow rate at an impeller inlet is used for a compressible fluid whose volume is variable between the impeller inlet and the impeller exit.

40 **[0008]** With regard to a blade profile, the inlet blade angle is determined by the assumed inlet velocity triangle at each spanwise location to match the inlet blade angle with the inlet flow angle. On the other hand, the exit blade angle is determined by the assumed exit velocity triangle at each spanwise location to satisfy the design head. The inlet and the exit velocity triangles are calculated from the meridional geometry and the design flow rate and the design head, but can be updated based on the results of flow calculation of the impeller. However, there are many degree of freedom as to a way of determining blade angle distribution which connect inlet and exit blade angles, and in effect the choice

of the blade angle distribution is left to designer's intuition.

[0009] There has been proposed many methods up to now in accordance with the approach which makes the impeller have a specific flow channel geometry to suppress the secondary flows. However, since the method of achieving the effect universally has not been sufficiently studied, design criterion of blade profile having many degrees of freedom has not been established. Therefore, the universal methods of suppressing the secondary flows under different design conditions and for the different specific speeds have not been established. Under these circumstances, the three-dimensional geometry of the impeller has been designed on the basis of variation of blade angle distribution of the impeller by trial and error to find the optimum profile of the impeller for suppressing the secondary flow.

[0010] Next, a conventional method of designing the three-dimensional geometry of the impeller on the basis of variation of blade angle distribution by trial and error will be described below in accordance with a flow chart in Fig. 3(A).

[0011] In the first step (step of determining meridional plane), the design specification is input to determine the meridional geometry and the number of blades of the impeller. Next, a plurality of surfaces of revolution is defined on a meridional flow passage, and the tangential co-ordinate f_0 of a blade camber line at a point on each of surfaces of revolution is specified based on the past experience. The location, where the tangential co-ordinate f_0 is specified, is selected at the leading edge or at the trailing edge of the impeller in many cases. Thus specified location of the tangential co-ordinate f_0 is referred as the stacking condition.

[0012] In the second step (step of determining blade angle distribution), the blade angle at the impeller inlet is determined from the meridional geometry of the impeller obtained by the first step and design flow rate. Next, the blade angle at the impeller exit is determined from the meridional geometry of the impeller obtained by the first step, and design head. A curve which connects smoothly the determined blade angle at the impeller inlet and the blade angle at the impeller exit is defined to determine the blade angle distribution along the location of non-dimensional meridional distance m .

[0013] In the third step (step of determining a blade profile), tangential co-ordinate (wrap angle) of the blade camber line in each of the locations of non-dimensional meridional distance m is determined by integrating $\partial f/\partial m = 1/(r \tan \beta)$ with the location of non-dimensional meridional distance m on the basis of blade angle distribution β between the impeller inlet and the impeller exit along each stream line in the location of non-dimensional meridional distance m , using stacking condition f_0 as initial value. The three-dimensional geometry of the impeller is determined by adding a certain thickness to the determined blade camber line to allow the blade to have a mechanical strength.

[0014] In the fourth step (step of evaluating flow fields), three-dimensional inviscid flow analysis which is a flow analysis without consideration of viscosity of fluid is applied to the three-dimensional geometry of the impeller determined by the third step, and a possibility of poor performance caused by a flow separation due to rapid deceleration of flow in the impeller is evaluated. In the case where it is judged that the pressure distribution in the impeller is not appropriate, after going back to the second step to modify the blade angle distribution, the steps from the second step to the fourth step are repeated until the expected result is achieved.

[0015] In case of suppressing the secondary flow by the above-mentioned conventional method of manufacturing the impeller, the following disadvantages are enumerated.

(1) In the fourth step, the criteria (including the dependence on the specific speed of the impeller) for judging whether optimum pressure distribution in the flow channel is achieved to suppress the secondary flow is uncertain. Though the state of generation of the secondary flows can be examined by the three-dimensional viscous flow analysis, enormous amount of calculations are required, thus optimization of the blade profile of the impeller by repeating the steps from the second step to the fourth step is practically infeasible.

(2) Although it is necessary to make the blade angle distribution proper in the second step, if the blade angle distribution which achieves the secondary flow suppression deviates greatly from conventional experience, it is difficult to assume favorable blade angle distribution. Therefore, in practice, it has been difficult to find by trial and error optimum blade profile of the impeller for suppressing the secondary flow.

[0016] However, recently, as a design method of a blade profile of the impeller, it is known that if a blade loading distribution is given, the three-dimensional geometry of the impeller which realizes the given blade loading distribution can be determined by using three-dimensional inverse design method which is published in the following literature.

[0017] Zangeneh, M., 1991, "A Compressible Three Dimensional Blade Design Method for Radial and Mixed Flow Turbomachinery Blades", International Journal of Numerical Methods in Fluids, Vol. 13, pp.599-624., Borges, J.E., 1990, "A Three-Dimensional Inverse Method for Turbomachinery: Part I - Theory", Transaction of the ASME, Journal of Turbomachinery, Vol.112, pp.346-354, Yang, Y.L., Tan, C.S. and Hawthorne, W.R., 1992, "Aerodynamic Design of Turbomachinery Blading in Three-Dimensional Flow: An Application to Radial Inflow Turbines", ASME Paper 92-GT-74, Dang, T.Q., 1993, "A Fully Three-Dimensional Inverse Method for Turbomachinery Blading in Transonic Flows", Transactions of the ASME, Journal of Turbomachinery, Vol. 115, pp.354-361, Borges, J.E., 1993 "A Proposed Through-Flow Inverse Method for the Design of Mixed-Flow Pumps", International Journal for Numerical Methods in Fluids, Vol. 17,

pp.1097-1114.

[0018] Most of the above methods design the blade shape based on the three-dimensional inviscid flow through the blade channels. However, the method described by Borges (1993) uses a more approximate Actuator Duct approach in which the flow field is assumed to be axisymmetric. Such an approximate approach can provide a very computationally efficient means of arriving at the blade geometry for a specified loading distribution. However, the errors in this approach become quite high for very highly loaded turbomachines such as centrifugal pumps. Incidentally, in none of these literature the inverse design method has been used for the purpose of suppression of secondary flows in an impeller.

[0019] It is apparent from the secondary flow theory that the secondary flow in the impeller results from the action of Coriolis force caused by the rotation of the impeller and the effects of the streamline curvature. The secondary flow in the impeller is divided broadly into two categories, one of which is blade-to-blade secondary flow generated along a shroud surface or a hub surface, the other of which is the meridional component of secondary flow generated along the pressure surface or the suction surface of a blade.

[0020] It is known that the blade-to-blade secondary flow can be minimized by making the blade profile to be back-swept. Regarding the other type of secondary flow, that is, the meridional component of secondary flow, it is difficult to weaken or eliminate it easily. If we wish to weaken or eliminate the meridional component of secondary flow, it is necessary to optimize the three-dimensional geometry of the flow channel very carefully.

[0021] The purpose of the present invention is to suppress the meridional component of secondary flow in a centrifugal or a mixed flow turbomachine.

[0022] As an example of a typical impeller in the turbomachinery to which the present invention is applied, the three-dimensional geometry of a closed type impeller is schematically shown in Figs. 1(A) and 1(B) in such a state that most part of shroud surface is removed. Fig. 1(A) is a perspective view partly in section, and Fig. 1(B) is a cross-sectional view taken along a line A-A' which is a meridional cross-sectional view. In Figs. 1(A) and 1(B), a hub surface 2 extends radially outwardly from a rotating shaft 1 so that it has a curved surface similar to a corn surface. A plurality of blades 3 are provided on the hub surface 2 so that they extend radially outward from the rotating shaft 1 and are disposed at equal intervals in the circumferential direction. The blade tip 3a of the blades 3 are covered with a shroud surface 4 as shown in Fig. 1(B). A flow channel is defined by two blades 3 in confrontation with each other, the hub surface 2 and the shroud surface 4 so that fluid flows from an impeller inlet 6a toward an impeller exit 6b. When the impeller 6 is rotated about an axis of the rotating shaft 1 at an angular velocity ω , fluid flowing into the flow channel from the impeller inlet 6a is delivered toward the impeller exit 6b of the impeller 6. In this case, the surface facing the rotational direction is the pressure surface 3b, and the opposite side of the pressure surface 3b is the suction surface 3c. In the case of open type impeller, there is no independent part for forming the shroud surface 4, but a casing (not shown in the drawing) for enclosing the impeller 6 serves as the shroud surface 4. Therefore, there is no basic fluid dynamical difference between the open type impeller and the closed type impeller in terms of the generation and the suppression of the meridional component of secondary flows, thus only the closed type impeller will be described below.

[0023] The impeller 6 having a plurality of blades 3 is incorporated as a main component, the rotating shaft 1 is coupled to a driving source, thereby jointly constituting a turbomachine. Fluid is introduced into the impeller inlet 6a through a suction pipe, pumped by the impeller 6 and discharged from the impeller exit 6b, and then delivered through a discharge pipe to the outside of the turbomachine.

[0024] The unsolved serious problem in connection with the impeller of turbomachine is the suppression of the meridional component of secondary flow. The mechanism of generation of meridional component of secondary flow, whose suppression is the purpose of this invention, is explained as follows:

[0025] As shown in Fig. 1(B), with regard to the relative flow, the reduced static pressure distribution, defined as $p^* = p - 0.5\rho u^2$, is formed by the action of a centrifugal force W^2/R due to streamline curvature of the main flow and the action of Coriolis force $2\omega W_\theta$ due to the rotation of the impeller, where W is the relative velocity of flow, R is the radius of streamline curvature, ω is the angular velocity of the impeller, W_θ is the component in the circumferential direction of W relative to the rotating shaft 1, p^* is reduced static pressure, p is static pressure, ρ is density of fluid, u is peripheral velocity at a certain radius r from the rotating shaft 1. The reduced static pressure p^* has such a distribution in which the pressure is high at the hub side and low at the shroud side, so that the pressure gradient balances the centrifugal force W^2/R and the Coriolis force $2\omega W_\theta$ directed toward the hub side.

[0026] In the boundary layer along the blade surface, since the relative velocity W is reduced in the boundary layer developing along the wall surface, the centrifugal force W^2/R and the Coriolis force $2\omega W_\theta$ acting on the fluid in the boundary layer become small. As a result, they cannot balance the reduced static pressure gradient of the main flow, and low energy fluid in the boundary layer flows towards an area of low reduced static pressure p^* , thus generating the meridional component of secondary flow. That is, as shown in broken lines on the pressure surface 3b and in solid lines on the suction surface 3c in Fig. 1(A), fluid moves along the blade surface from the hub side towards the shroud side on the pressure surface 3b and the suction surface 3c forming meridional component of secondary flow.

[0027] The meridional component of secondary flow is generated on both surfaces of the suction surface 3c and the

pressure surface 3b. In general, since the boundary layer on the suction surface 3c is thicker than that on the pressure surface 3b, the secondary flow on the suction surface 3c has a greater influence on performance characteristics of turbomachinery. The purpose of the present invention is to suppress the meridional component of secondary flow on the suction surface of the blade.

5 **[0028]** When low energy fluid in the boundary layer moves from the hub side to the shroud side, fluid flow is formed from the shroud side to the hub side at around the midpoint location to compensate for fluid flow rate which has moved. As a result, as shown schematically in Fig. 2(B) which is a cross-sectional view taken along a line B-B' in Fig. 2(A), a pair of vortices which have a different swirl direction from each other are formed in the flow channel between two blades as the flow goes towards exit. These vortices are referred to as secondary vortices. Low energy fluid in the flow channel is accumulated due to these vortices at a certain location of the impeller towards the exit where the reduced static pressure p^* is lowest, and this low energy fluid is mixed with fluid which flows steadily in the flow channel, resulting in generation of a great flow loss.

10 **[0029]** Furthermore, when the non-uniform flow generated by insufficient mixing of a low relative velocity (high loss) fluid and a high relative velocity (high loss) fluid is discharged to the downstream flow channel of the blades, a great flow loss is generated when both fluids are mixed.

15 **[0030]** Such a non-uniform flow leaving the impeller makes the velocity triangle unfavorable at the inlet of the diffuser and causes flow separation on diffuser vanes or a reverse flow within a vaneless diffuser, resulting in a substantial decrease of the overall performance of the turbomachine.

20 **[0031]** Furthermore, in the area of high loss fluid accumulated at a certain location in the flow channel, a large scale reverse flow is liable to occur, thus producing a positively sloped characteristics curve. As a result, surging, vibration, noise and the like are generated, and the turbomachinery cannot be stably operated especially at partial flow rate.

25 **[0032]** Therefore, in order to improve the performance of centrifugal or mixed flow turbomachinery and realize stable operation of turbomachinery, it is necessary to design the three-dimensional geometry of the flow channel for suppressing the secondary flow as much as possible, whereby the formation of secondary vortices, the resulting non-uniform flow, and large scale flow separation or the like may be prevented.

Disclosure of Invention

30 **[0033]** It is therefore an object of the present invention to overcome the drawbacks of increase of loss and unstable operation of turbomachinery caused by insufficient suppression of meridional component of secondary flow in the impeller, and to provide the following four design aspects by which the blade profile of the impeller in the turbomachinery is designed using the three-dimensional inverse design method and the impeller having such blade profile is manufactured to thus reduce the above loss and improve stability of operation of the turbomachinery.

35 **[0034]** According to the present invention, there is provided a turbo machine having an impeller with a plurality of blades supported by a hub on which said blades are circumferentially spaced and covered by a shroud surface which forms an outer boundary to flow of fluid in a flow passage defining a flow direction between two adjacent blades, characterized in that:

40 said impeller has a configuration such that one of a reduced static pressure difference ΔC_p and a relative Mach number difference ΔM between the hub and the shroud on the suction surface of the blade shows a remarkably decreasing tendency along the location of non-dimensional meridional distance m toward the impeller exit and is selected to be not less than a specified value which is dependent on a specific speed N_s of the turbomachines, herein specific speed N_s is defined as $N_s = NQ^{0.5}/H^{0.75}$, where N is the rotational speed in revolutions per minute, Q is the flow rate at an impeller inlet in cubic meters per minute, and H is the head in meters representing fluid energy which is imparted to the fluid by the turbomachine;

45 said remarkably decreasing tendency of ΔC_p for the turbomachine handling incompressible fluid is arranged such that the reduced static pressure difference between a minimum value ΔC_{pm} of reduced static pressure difference ΔC_p and a value $\Delta C_{pm-0.4}$ of reduced static pressure difference ΔC_p at the location corresponding to non-dimensional meridional distance $m_{m-0.4}$ obtained by subtracting non-dimensional meridional distance 0.4 from non-dimensional meridional distance m_m representing said minimum value ΔC_{pm} is selected to be

50 not less than 0.20 at said specific speed N_s of not more than 280,
not less than 0.28 at said specific speed N_s of not more than 400, and
not less than 0.35 at said specific speed N_s of not more than 560; and

55 said remarkably decreasing tendency of ΔM for the turbomachine handling compressible fluid is arranged such that relative Mach number difference between minimum value ΔM_m of the relative Mach number difference ΔM and a value $\Delta M_{m-0.4}$ of the relative Mach number difference ΔM at the location corresponding to non-dimensional meridional distance $M_{m-0.4}$ obtained by subtracting non-dimensional meridional distance 0.4 from non-dimensional meridional distance M_2 representing said minimum value ΔM_m is selected to be not less than 0.23 at said specific

speed of not more than 488.

[0035] The present invention also provides a method of manufacturing a turbomachine having an impeller with a plurality of blades supported by a hub on which said blades are circumferentially spaced and covered by a shroud surface which forms an outer boundary to flow of fluid in a flow passage defining a flow direction between two adjacent blades, comprising:

a first step of selecting meridional geometry and the number of blades of the impeller using design specification as input data, defining a plurality of surface of revolution in a meridional flow channel, and determining stacking condition f_0 ;

a second step of determining distribution of blade loading rV_θ along non-dimensional meridional distance m by selecting a shape of the blade loading distribution $\delta(rV_\theta)/\delta m$ which has a peak on the shroud surface in the first half of the location of non-meridional distance m and a peak on the hub surface in the latter half of the location of non-dimensional meridional distance, adjusting a value obtained by integrating the blade loading distribution along the non-dimensional meridional distance m so as to satisfy design head of the impeller;

a third step of determining three-dimensional geometry of the impeller by integrating

$$\{(\bar{V} z + v_{zb1})\delta f/\delta z\} + \{(\bar{V} r + v_{rb1})\delta f/\delta r\} = \{(r\bar{V}_\theta)/r^2\} + \{(v_{ob1})/r\} - \omega$$

along non-dimensional meridional distance m using stacking condition f_0 as initial value to determine tangential co-ordinate f of the blade camber line in non-dimensional meridional distance m and adding a certain thickness to the determined value to allow the blade to have required mechanical strength;

a fourth step of judging whether one of the distribution of reduced static pressure difference ΔC_p and the distribution of a relative Mach number difference ΔM along non-dimensional meridional distance m obtained by the third step is suitable for suppressing the secondary flow in the impeller or not;

a fifth step of evaluating possibility of poor performance caused by at least flow separation in the impeller determined by the third step, evaluating secondary flow in the impeller by a secondary flow parameter, and after going back to the second step to modify the blade loading distribution on the basis of the above evaluation, repeating the above steps until the expected result is achieved;

wherein one of a reduced static pressure difference ΔC_p and a relative Mach number difference ΔM between the hub and the shroud on the suction surface of the blade shows a remarkably decreasing tendency along the location of non-dimensional meridional distance m toward the impeller exit and is selected to be not less than a specified value which is dependent on a specific speed N_s of the turbomachines, herein specific speed N_s is defined as $N_s = NQ^{0.5}/H^{0.75}$, where N is the rotational speed in revolution per minutes, Q is the flow rate at an impeller inlet in cubic meter per minutes, and H is the head in meter representing fluid energy which is imparted to the fluid by the turbomachine;

said remarkably decreasing tendency of ΔC_p for the turbomachine handling incompressible fluid is arranged such that the reduced static pressure difference between a minimum value ΔC_{pm} of reduced static pressure difference ΔC_p and a value $\Delta C_{pm-0.4}$ of reduced static pressure difference ΔC_p at the location corresponding to non-dimensional meridional distance $m_{m-0.4}$ obtained by subtracting non-dimensional meridional distance 0.4 from non-dimensional meridional distance m_m representing said minimum value ΔC_{pm} is selected to be

- not less than 0.20 at said specific speed N_s of not more than 280,
- not less than 0.28 at said specific speed N_s of not more than 400, and
- not less than 0.35 at said specific speed N_s of not more than 560; and

said remarkably decreasing tendency of ΔM for the turbomachine handling compressible fluid is arranged such that relative Mach difference between a minimum value ΔM_m of the relative Mach number difference ΔM and a value $\Delta M_{m-0.4}$ of the relative Mach number difference ΔM at the location corresponding to non-dimensional meridional distance $m_{m-0.4}$ obtained by subtracting non-dimensional meridional distance 0.4 from non-dimensional meridional distance m_m representing said minimum value ΔM_m is selected to be not less than 0.23 at said specific speed of not more than 488.

[0036] Further, in order to prevent a flow separation at the location after non-dimensional meridional distance $m_{m-0.4}$ at which the value $\Delta M_{m-0.4}$ of relative Mach number difference ΔM emerges, the Mach number slope at the shroud side MS-s may be selected to be not less than -0.8 as the lower limit of the Mach number slope at the shroud side MS-S, lim . Here, the Mach number slope at the shroud side MS-S on the suction surface of the blade is defined as a gradient of Mach number on the shroud surface at the location between the non-dimensional meridional distance m_m representing the above minimum value Δm_m of relative Mach number difference ΔM and the non-dimensional meridional distance $m_{m-0.4}$ obtained by subtracting non-dimensional meridional distance 0.4 from non-dimensional merid-

ional distance mm representing the above minimum value.

[0037] By selecting specifically this Mach number slope at the shroud side MS-s on the suction of the blade, the flow separation can be prevented in the downstream side of the location of non-dimensional meridional distance mm-0.4. In order to prevent the flow separation in the overall area of non-dimensional meridional distance m from the impeller inlet to the impeller exit, especially, in the upstream side of the location of non-dimensional meridional distance mm-0.4, the non-dimensional meridional distance mm representing the minimum value ΔMm of relative Mach number ΔM is preferably selected to be in the range of non-dimensional meridional distance m-0.8-1.0.

[0038] According to the first aspect of the present invention, while selecting properly by trial and error the distribution of the meridional derivative of $r\bar{V}_\theta$, i.e. blade loading distribution $\partial(r\bar{V}_\theta)/\partial m$ along the meridional distance m on the basis of the known close relationship between the pressure coefficient Cp and the angular momentum $r\bar{V}_\theta$, the pressure coefficient Cp is increased or decreased. And, by utilizing the known three-dimensional inverse design method using the blade loading distribution as input data, the impeller is designed so that the above-mentioned characteristic decreasing tendency in the reduced static pressure difference ΔCp or the relative Mach number difference ΔM between the hub and the shroud on the suction surface of the blade is realised, and further the above-mentioned characteristic limit in the pressure coefficient slope at the shroud side CPS-s or the Mach number slope at the shroud side MS-s on the suction surface of the blade is realised.

[0039] In the turbomachinery having the impeller with the three-dimensional geometry obtained by the above design method, the meridional component of secondary flow can be remarkably suppressed around and after the location of non-dimensional meridional distance mm-0.4 where the reduced static pressure difference ΔCp or the relative Mach number difference ΔM shows a remarkably decreasing tendency toward the impeller exit. As a result, the meridional component of secondary flow can be effectively suppressed in the overall area of the impeller.

Brief Description of Drawings

[0040]

Figs. 1 and 2 are views for explaining the background art;

Figs. 1(A) through 1(E) are views for explaining meridional component of secondary flow in three-dimensional geometry of a closed type impeller, Fig. 1(A) is a perspective view partly in section, Fig 1(B) is a meridional cross-sectional view taken along line A-A' of Fig. 1(A), Fig 1(C) is a view for explaining a computational mesh in three-dimensional viscous calculation, Fig. 1(D) is a perspective view showing midspan and midpitch of the impeller, and Fig. 1(E) is a view showing a blade profile of the impeller;

Figs. 2(A) and 2(B) are views for explaining secondary vortices caused by meridional component of secondary flow in the closed type impeller, Fig. 2(A) is a perspective view partly in section, and Fig. 2(B) is a cross-sectional view taken along line B-B' of Fig. 2(A);

Figs. 3(A) and 3(B) are flow charts of numerical analysis by a computer to determine a three-dimensional shape of the impeller in the turbomachinery, Fig. 3(A) is a flow chart showing a conventional design method of designing the three-dimensional geometry of the impeller, and Fig. 3(B) is a flow chart showing a three-dimensional inverse design method which has been put to practical use recently, according to the present invention;

Fig. 4 is a graph showing verification data plotted on the plane defined by a vertical axis representing the pressure coefficient slope at the shroud side CPS-s and a horizontal axis representing the pressure coefficient slope at the hub side CPS-h, and further showing boundary lines defined by specific speeds N_s and the lower limit of the pressure coefficient slope at the shroud side $CPS-s_{LIM}$;

Fig. 5 is a graph showing verification data plotted on the plane defined by a vertical axis representing the Mach number slope at the shroud side MS-s and a horizontal axis representing the Mach number slope at the hub side MS-h, and further showing boundary lines defined by specific speeds N_s and the lower limit of the Mach number slope at the shroud side $MS-s_{LIM}$;

Fig. 6 is a graph showing verification data plotted on the plane defined by a vertical axis representing the difference D^* between a minimum value ΔCp^*m of the normalized reduced static pressure difference ΔCp^* and a value $\Delta Cp^*_{m-0.4}$ of the normalized reduced static pressure difference ΔCp^* at the location corresponding to non-dimensional meridional distance mm-0.4 obtained by subtracting non-dimensional meridional distance 0.4 from non-dimensional meridional distance mm representing the above minimum value ΔCp^*m and a horizontal axis representing a specific speed N_s , and further showing boundary lines defined by specific speeds N_s , thereby expressing the above difference D^* as a function of the specific speeds N_s ;

Fig. 7(A) is a table showing the pressure coefficient slope at the shroud side CPS-s and the pressure coefficient slope at the hub side CPS-h read from characteristic graphs in verification examples, and MSF-angle calculated as secondary flow parameter, and Fig. 7(B) is a table showing the difference D^* on the basis of the normalized pressure coefficient Cp^* shown in the same manner as Fig. 7(A);

Figs. 8 through 22 are characteristic graphs showing the distribution of the pressure coefficient C_p along non-dimensional meridional distance m of the blade, Fig. 8 is a graph showing a verification example "A", Fig. 9 is a graph showing a verification example "B", Fig. 10 is a graph showing a verification example "C", Fig. 11 is a graph showing a verification example "D", Fig. 12 is a graph showing a verification example "E", Fig. 13 is a graph showing a verification example "F", Fig. 14 is a graph showing a verification example "G", Fig. 15 is a graph showing a verification example "H", Fig. 16 is a graph showing a verification example "I", Fig. 17 is a graph showing a verification example "J", Fig. 18 is a graph showing a verification example "K", Fig. 19 is a graph showing a verification example "L", Fig. 20 is a graph showing a verification example "M", Fig. 21 is a graph showing a verification example "N", and Fig. 22 is a graph showing a verification example "O";

Fig. 23 is a flow vector diagram showing the state of flow separation in the verification example "O";

Figs. 24 through Fig. 29 are characteristic graphs showing the distribution of the Mach number along non-dimensional meridional distance m of the blade, Fig. 24 is a graph showing a verification example "P", Fig. 25 is a graph showing a verification example "Q", Fig. 26 is a graph showing a verification example "R", Fig. 27 is a graph showing a verification example "S", Fig. 28 is a graph showing a verification example "T", and Fig. 29 is a graph showing a verification example "U";

Fig. 30 is a flow vector diagram showing the state of flow separation in the verification example "U".

Best Mode for Carrying Out the Invention

[0041] An embodiment according to the first aspect of the present invention will be described below.

[0042] The influence of viscosity can be neglected for main flow of the relative flow in the flow channels of an impeller, therefore the following formula is approximately satisfied in incompressible flow as in a liquid pump.

$$P_0^* = p^* + 0.5\rho W^2 = \text{constant}$$

where P_0^* is rotary stagnation pressure at the upstream of the impeller.

[0044] Next, as non-dimensional quantity of reduced static pressure p^* on the blade surface, pressure coefficient C_p is defined by the following equation:

$$C_p = (P_0^* - p^*) / (0.5\rho Ut^2) = (W/Ut)^2$$

where Ut represents the mean peripheral speed at the impeller exit.

[0045] As is apparent from the above equation, the pressure coefficient C_p is large at the shroud where reduced static pressure p^* is low, and is small at the hub where reduced static pressure p^* is high. As mentioned above, since the meridional component of secondary flow on the blade suction surface is directed to the shroud side having low reduced static pressure p^* from the hub side having high reduced static pressure p^* , suppression of meridional component of secondary flow can be expected by reducing pressure difference ΔC_p between them. Incidentally, in case of incompressible fluid, the pressure coefficient C_p is equal to $(W/Ut)^2$, where W is relative velocity. In compressible fluid as in a compressor, the physical variable being related to the behavior of secondary flow is relative Mach number. In order to simplify the description, only the distribution of the pressure coefficient C_p will be described below. The influence of distribution of the pressure coefficient C_p in incompressible flow upon meridional component of secondary flow is equivalent to that of the relative Mach number M in compressible flow. Here, static pressure p or relative Mach number M is obtained through three-dimensional steady inviscid flow calculation.

[0046] Since the boundary layers on the blade surfaces which develop along the wall of the flow channel in the impeller increase their thickness cumulatively from the impeller inlet toward the impeller exit, the present invention proposes the structure for suppressing meridional component of secondary flow on the suction surface of the blade, considering distribution of the pressure coefficient C_p mainly in the latter half of the impeller. That is, the blade profile is designed so as to have the pressure distribution so that the pressure difference ΔC_p between the shroud side and the hub side on the suction surface shows a remarkably decreasing tendency along the location of non-dimensional meridional distance m toward the impeller exit.

[0047] Fig. 8 is a characteristic graph showing distribution of the pressure coefficient C_p obtained by the three-dimensional steady inviscid flow calculations, and thus the reduced static pressure difference ΔC_p of a pump according to a best mode of the first aspect of the present invention. In Fig. 8, the vertical axis represents the pressure coefficient C_p , and the horizontal axis represents the location between non-dimensional meridional distance $m=0$ (impeller inlet) and non-dimensional meridional distance $m=1.0$ (impeller exit). In Fig. 8, a solid curve at the upper part of the graph shows a pressure coefficient curve representing values of the pressure coefficient on the suction surface of the blade at the shroud side along the location of non-dimensional meridional distance m , and an alternative long and short dash curve extending substantially along the above solid line shows values of the pressure coefficient at the midpitch location on the shroud surface.

[0048] On the other hand, in Fig. 8, a solid curve at the lower part of the graph shows a pressure coefficient curve representing values of the pressure coefficient on the suction surface of the blade at the hub side along the location of non-dimensional meridional distance m , and an alternative long and short dash curve extending substantially along the above solid line shows values of the pressure coefficient at the midpitch location on the hub surface.

[0049] Broken line curves show the pressure coefficient on the pressure surface of the blade at the shroud and hub sides, respectively. These curves are not directly related to the present invention, but are depicted for reference.

[0050] In Fig. 8, the distance between the solid curves adjacent to each other along the vertical axis, i.e. the difference between a value on the pressure coefficient curve at the shroud side and a value on the pressure coefficient curve at the hub side at the same location of non-dimensional meridional distance m corresponds to the reduced static pressure difference ΔC_p . The location of non-dimensional meridional distance mm at which a minimum value $\Delta C_{p,m}$ (in case of a negative value, a maximum value of absolute value) of reduced static pressure difference ΔC_p emerges is defined on the horizontal axis, and the location which approaches the impeller inlet ($m=0$) by non-dimensional meridional distance 0.4 from the location of non-dimensional meridional distance mm , that is, the location corresponding to non-dimensional meridional distance $mm-0.4$ obtained by subtracting non-dimensional meridional distance 0.4 from non-dimensional meridional distance mm representing the above minimum value $\Delta C_{p,m}$ is defined.

[0051] Here, the gradient of inclined straight line which connects the value $C_{p_{s,m-0.4}}$ on the pressure coefficient curve on the shroud surface at the location of non-dimensional meridional distance $mm-0.4$ and the value $C_{p_{s,m}}$ on the pressure coefficient curve on the shroud surface at the location of non-dimensional meridional distance mm , i.e. $(C_{p_{s,m}} - C_{p_{s,m-0.4}})/0.4$ is defined as a pressure coefficient slope at the shroud side CPS-s. In the example of Fig. 8, the pressure coefficient slope at the shroud side CPS-s is negative. Similarly, the gradient of straight line which connects the value $C_{p_{h,m-0.4}}$ on the pressure coefficient curve on the hub surface at the location of non-dimensional meridional distance $mm-0.4$ and the value $C_{p_{h,m}}$ on the pressure coefficient curve on the hub surface at the location of non-dimensional meridional distance mm , i.e. $(C_{p_{h,m}} - C_{p_{h,m-0.4}})/0.4$ is defined as a pressure coefficient gradient at the hub side CPS-h. In the example of Fig. 8, the pressure coefficient slope at the hub side CPS-h is positive.

[0052] It was confirmed on the basis of many verification examples by the inventors of the present invention that the difference between the value on the pressure coefficient curve at the shroud side at the location of non-dimensional meridional distance $mm-0.4$ and the value on the pressure coefficient curve at the hub side at the location of non-dimensional meridional distance $mm-0.4$, that is, the difference D between the reduced static pressure difference $\Delta C_{p_{m-0.4}}$ at the location of non-dimensional distance $mm-0.4$ and the minimum value $\Delta C_{p,m}$ of the reduced static pressure difference ΔC_p is the essential factor which govern suppression of the secondary flow in the impeller of the turbomachinery. Here, the difference D is derived from cooperative contribution of the pressure coefficient slope at the shroud side CPS-s and the pressure coefficient slope at the hub side CPS-h, thus the differences D between the reduced static pressure difference $\Delta C_{p_{m-0.4}}$ at the location of non-dimensional meridional distance $mm-0.4$ and the minimum value $\Delta C_{p,m}$ of the reduced static pressure difference ΔC_p in principal verification examples were plotted in Fig. 4 on the plane defined by horizontal and vertical axes representing the above respective slopes or gradients. In Fig. 4, the vertical axis represents the pressure coefficient slope at the shroud side CPS-s, and the horizontal axis represents the pressure coefficient slope at the hub side CPS-h. In Fig. 4, Δ represent verification examples of pumps of a specific speed $N_s=280$, \square represent verification examples of pumps of a specific speed $N_s=400$, and \circ represent verification examples of pumps of a specific speed $N_s=560$. Further, open symbols (Δ , \square , \circ) represent adaptation to the quantitative criterion (describe latter) of judgement about suppression of the secondary flow, and solid symbols (\blacktriangle , \blacksquare , \bullet) represent nonadaptation to the above criterion.

[0053] Fig. 7(A) is a table showing data in principal verification examples. Fig. 7(A) includes six verification examples A, B, C, D, 1 and 2 in pumps of a specific speed $N_s=280$. Concerning four examples A, B, C and D, four pairs of data as to values of the pressure coefficient slope at the shroud side CPS-s and the pressure coefficient slope at the hub side CPS-h were read from the pressure coefficient curves of the verification examples shown in Figs. 8 through 11 in the order of A, B, C and D, and four Δ symbols were plotted on the plane between two axes from the readings. Concerning two examples 1 and 2, the pressure coefficient curves in the verification examples are not shown, but the resultant data were represented for reference as a part of large amount of other verification examples.

[0054] Four verification examples A, B, C and D in pumps of a specific speed $N_s=400$ are the same as the above. Four pairs of data as to values of the pressure coefficient slope at the shroud side CPS-s and the pressure coefficient slope at the hub side CPS-h were read from the pressure coefficient curves of the verification examples shown in Figs. 12 through 15 in the order of E, F, G and H, and four \square symbols were plotted in Fig. 4. Further, six verification examples I, J, K, L, M and N in pumps of a specific speed $N_s=560$ are the same as the above. Data concerning values of the pressure coefficient slope at the shroud side CPS-s and the pressure coefficient slope at the hub side CPS-h were read from the pressure coefficient curves of the verification examples shown in Figs. 16 through 21 in the order of I, J, K, L, M and N, and six \circ symbols were plotted in Fig. 4. Concerning verification examples, 3, 4, 5, 6 and O, the resultant data were represented for reference.

[0055] In the plotted data in Fig. 4, as described above, open and solid symbols represent adaptation or nonadap-

tation to the quantitative criterion of judgement about suppression of the secondary flow. The quantitative criterion of judgement will be described below.

[0056] Fig. 1(C) is an explanatory view used for the three-dimensional viscous flow calculation and showing the relationship between the computational meshes inside the bladed region and the secondary flow angle α defined in each of the computational meshes. Since the secondary flow is defined as flow which has a velocity component deviating from the direction of the computational mesh, the computational mesh to be used as a basis is required to have a certain regularity. That is, mesh is divided regularly (i.e. mesh division is applied at the same number of mesh points and the same ratio of mesh spacing) between the blade leading edge and the blade trailing edge in J direction on the hub and the shroud surfaces, and meshes of the spanwise direction (K direction) in each J location which connects two corresponding points on the hub surface and the shroud surface are divided regularly, whereby the computational mesh is defined over the entire bladed region. Such computational mesh is generally used in the three-dimensional viscous calculation.

[0057] MSF-angle used as the quantitative criterion of judgement about suppression of the secondary flow is expressed by the following equation.

$$\text{MSF-angle} = \left[\int_{0.15}^{1.0} \int_{0.0}^{1.0} \alpha \cdot \rho V_m \cos \alpha \cdot ds \cdot dm \right]_{ss} / \left[\int_{0.15}^{1.0} \int_{0.0}^{1.0} \rho V_m \cos \alpha \cdot ds \cdot dm \right]_{ss}$$

where α is an angle between the tangential direction along the streamwise mesh (J direction) and the direction of meridional velocity vector at the location near the suction surface of the blade in each computational mesh in the bladed region in Fig. 1(C);

V_m is meridional velocity;

s is non-dimensional meridional span length in K direction, s being 0 on the hub surface and 1 on the shroud surface on each of Jth Quasi-orthogonal line (mesh line of K direction);

m is non-dimensional meridional distance in J direction, m being 0 at the blade leading edge and 1 at the blade trailing edge on each of Kth stream surface;

$[\]_{ss}$ is integrated value in the first mesh from the suction surface of the blade.

[0058] That is, MSF-angle is defined as mass-averaged value of the magnitude of the flow deviation angle from the streamwise mesh direction over the entire suction surface of the blade.

[0059] There is a tendency that when flow which has impinged on the blade at the impeller inlet portion moves around the blade leading edge, a part of flow deviates from the mesh direction. Since this deviation angle has no meaning in the secondary flow caused by viscous action in the boundary layer on the blade surface, in order to eliminate the influence of the above deviating flow, integration is made excluding the region between non-dimensional meridional distance $m=0.0$ and $m=0.15$ in which the boundary layer is thin.

[0060] In Fig. 7(A), the values of MSF-angle which were calculated by the above equation, the pressure coefficient slope at the shroud side CPS-s and the pressure coefficient slope at the hub side CPS-h in verification examples are shown.

[0061] On the other hand, the values of MSF-angle in a large amount of verification examples have been calculated by the same manner, and the relationship between the values of MSF-angle calculated in the verification examples and lowering of performance caused by the secondary flow in the verification examples has been studied by the inventors of the present invention. As a result, it was confirmed that as the quantitative criterion of judgement about the suppression of the secondary flow, the selection of the following MSF-angle is appropriate for each of the groups having similar number of mesh points and the specific speed.

[0062] MSF-angle as the criterion of judgement is 18 degrees in the pump of the specific speed $N_s=280$.

[0063] MSF-angle as the criterion of judgement is 15 degrees in the pump of the specific speed $N_s=400$.

[0064] MSF-angle as the criterion of judgement is 25 degrees in the pump of the specific speed $N_s=560$.

[0065] MSF-angle as the criterion of judgement is 15 degrees in the compressor of the specific speed $N_s=488$.

[0066] By comparing the values of MSF-angle shown in Fig. 7(A) representing the magnitude of secondary flow which is expressed quantitatively in each of verification examples with the confirmed value of MSF-angle for each of the groups as the quantitative criterion of judgement about the action of the secondary flow suppression, the value of MSF-angle in each of verification example equal to or larger than the value of MSF-angle as the criterion of judgement means nonadaptation to the above criterion of judgement (insufficient action of secondary flow suppression), and the

value of MSF-angle in each of verification example smaller than the value of MSF-angle as the criterion of judgement means adaptation to the above criterion of judgement (sufficient action of secondary-flow suppression). The data of the nonadaptation are shown by solid symbols, and the data of the adaptation are shown by open symbols in Fig. 4.

[0067] As shown in Fig. 4, a boundary line between data area of solid symbols which show nonadaptation to the criterion and data area of open symbols which show adaptation to the criterion can be drawn on the basis of data plotted in Fig. 4 for each of specific speeds N_s . In the drawing, the three positively sloped straight lines are boundary lines which correspond to the specific speeds $N_s=280$, $N_s=400$, and $N_s=560$, respectively. In each of the specific speeds N_s , data area located at the lower right side of the boundary line corresponds to data area of adaptation to the criterion. By further examination of the boundary line, each of data on the boundary line is such that the difference between values of the pressure coefficient slope at the shroud side CPS-s positioned along the vertical axis and values of the pressure coefficient slope at the hub side CPS-h positioned along the horizontal axis is maintained at a constant value. That is, the boundary line concerning the specific speed $N_s=280$ corresponds to the inclined straight line representing (the value of the pressure coefficient slope at the hub side CPS-h) - (the value of the pressure coefficient slope at the shroud side CPS-s) = $0.2/0.4 = 0.5$. Therefore, as shown in Fig. 8, this means that the difference D_{280} between a minimum value ΔC_{pm} of the reduced static pressure difference ΔC_p and a value $\Delta C_{p_{m-0.4}}$ of the reduced static pressure difference ΔC_p at the location corresponding to non-dimensional meridional distance $mm-0.4$ obtained by subtracting non-dimensional meridional distance 0.4 from non-dimensional meridional distance mm representing the minimum value ΔC_{pm} is maintained to be 0.20 . Therefore, concerning data of the specific speed $N_s=280$, the data in which the difference D_{280} is not less than 0.2 are plotted by open symbols in the data area of adaptation to the criterion located at the lower right side of the boundary line concerning the specific speed $N_s=280$. Thus, the impeller in which the difference D_{280} is not less than 0.2 is suitable for suppression of the secondary flow.

[0068] The boundary line concerning the specific speed $N_s=400$ corresponds to the inclined straight line representing (the value of the pressure coefficient slope at the hub side CPS-h) - (the value of the pressure coefficient slope at the shroud side CPS-s) = $0.28/0.4 = 0.7$. It can be said that this case is the same tendency as that of the specific speed $N_s=280$. Therefore, the impeller in which the difference D_{400} is not less than 0.28 is suitable for suppression of the secondary flow.

[0069] Further, the boundary line concerning the specific speed $N_s=560$ corresponds to the inclined straight line representing (the value of the pressure coefficient slope at the hub side CPS-h) - (the value of the pressure coefficient slope at the shroud side CPS-s) = $0.35/0.4 = 0.87$. It can be said that this case is also the same tendency as of the specific speed $N_s=280$. Therefore, the impeller in which the difference D_{560} is not less than 0.35 is suitable for suppression of the secondary flow.

[0070] As is apparent from the above description, data area of open symbols which are suitable for suppression of the secondary flow on the plane between the pressure coefficient slope at the shroud side CPS-s and the pressure coefficient slope at the hub side CPS-h means that the difference D between $\Delta C_{p_{m-0.4}}$ at the location of non-dimensional meridional distance $mm-0.4$ and the minimum value ΔC_{pm} of the reduced static pressure difference ΔC_p at the location of non-dimensional meridional distance mm can not be less than a certain value which is dependent on the criterion of judgement about suppression of the secondary flow. The value of the difference D is the result of cooperative contribution of the value of the pressure coefficient slope at the shroud side CPS-s on the vertical axis on the boundary line and the value of the pressure coefficient slope at the hub side CPS-h on the horizontal axis. The degree of contribution of both slopes varies in a wide range; there are three cases, i.e. the first case (1) which is largely dependent on the decreasing tendency of the pressure coefficient slope at the shroud side, the second case (2) which is dependent on the increasing tendency of the pressure coefficient slope at the hub side, and the third case (3) which is dependent on moderate harmonization of the decreasing tendency and the increasing tendency of both slopes. However, it was confirmed by the inventors of the present invention that as shown in Fig. 8, there exists a lower limit of the pressure coefficient slope at the shroud side CPS-s, LIM having a lower limit of negative value in the aft part from the location of non-dimensional meridional distance $mm-0.4$ to the impeller exit ($m=1.0$), and in the case where the formation of the difference D is dependent largely on the value of the pressure coefficient slope at the shroud side CPS-s less than the lower limit of the pressure coefficient slope at the shroud side CPS-s, LIM , the flow separation is occurred in the aft part from the location of non-dimensional meridional distance $mm-0.4$ to the impeller exit ($m=1.0$), generating significant reduction in head and efficiency.

[0071] The lower limit of the pressure coefficient slope at the shroud side CPS-s, LIM thus confirmed is -1.3 , and this is proved by the fact that the horizontal straight line, which defines data area generating flow separation and including three verification examples, 5, 6, and 0 at the lower side of the line, can be drawn. As an example, Fig. 23 is a flow vector diagram showing the state of flow separation in the verification example of O.

[0072] It was confirmed by the inventors of the present invention that the flow separation emerges in the aft part from the location of non-dimensional meridional distance $mm-0.4$ to the impeller exit ($m=1.0$) when CPS-s is less than the lower limit of CPS-s, LIM , but there exists another lower limit in the fore part of the blade toward the impeller inlet ($m=0$) different from the lower limit of the pressure coefficient slope at the shroud side CPS-s, LIM in the aft part from the

location of non-dimensional meridional distance $m=0.4$. In order to prevent flow separation caused by the steep pressure coefficient slope at the shroud side in the fore part of the location toward the impeller inlet ($m=0$), the location of non-dimensional meridional distance m at which the minimum value ΔC_{pm} of the reduced static pressure difference ΔC_p emerges is preferably selected to be in the range of non-dimensional meridional distance $m=0.8-1.0$, i.e. in the aft part toward the impeller exit ($m=1.0$).

[0073] Further, in the lower part of Fig. 7(A), concerning compressor of a specific speed $N_s=488$, the values of Mach number slope at the shroud side $MS-s$, the values of Mach number slope at the hub side $MS-h$ and the values of MSF-angle are shown for eight examples of P, 9, Q, R, S, T, U and 10. The data of verification examples were plotted on the plane of Fig. 5 corresponding to that of Fig. 4 in the same manner as Fig. 4.

[0074] As described above, in compressors which handle compressible fluid, it is known that the pressure coefficient slope at the shroud side $CPS-s$ and the pressure coefficient slope at the hub side $CPS-h$ correspond to the Mach number slope at the shroud side $MS-s$ and the Mach number slope at the hub side $MS-h$, respectively. The plane in Fig. 5 is defined by a vertical axis representing the Mach number slope at the shroud side $MS-s$ and a horizontal line representing the Mach number slope at the hub side $MS-h$.

[0075] From a large amount of verification data including principal verification examples plotted on the plane of Fig. 5, as a boundary line concerning a compressor of a specific speed $N_s=488$, an inclined straight line representing (the value of the Mach number slope at the hub side $MS-h$) - (the value of the Mach number slope at the shroud side $MS-s$) = $(0.23/0.4) = 0.575$ can be drawn, and data area located at the lower right side of the boundary line corresponds to data area of adaptation to the criterion of judgement about suppression of the secondary flow.

[0076] This means that in the compressor of a specific speed $N_s=488$, the difference MD_{488} between a minimum value ΔM_m of the reduced static pressure difference ΔM and a value $\Delta M_{m=0.4}$ of the reduced static pressure difference ΔM at the location corresponding to non-dimensional meridional distance $m=0.4$ obtained by subtracting non-dimensional meridional distance 0.4 from non-dimensional meridional distance m representing the minimum value ΔM_m is maintained to be 0.23. Therefore, it was confirmed from a large amount of verification examples that the impeller in which the difference MD_{488} is not less than 0.23 and which corresponds to data area shown by open symbols is suitable for suppression of the secondary flow.

[0077] However, it was confirmed by the inventors of the present invention that there exists a lower limit of the Mach number slope at the shroud side $MS-s_{LIM}$ and in the case where the value of the Mach number slope at the shroud side $MS-s$ is less than the lower limit of the Mach number slope at the shroud side $MS-s_{LIM}$, the flow separation is generated in the aft part from the location of non-dimensional meridional distance $m=0.4$ to the impeller exit ($m=1.0$), generating significant reduction in head and efficiency.

[0078] The lower limit of the pressure coefficient slope at the shroud side $CPS-s_{LIM}$ thus confirmed is -0.8 in the compressor of the specific speed $N_s=488$, and this is proved by the fact that the horizontal straight line, which defines data area generating flow separation and including two verification examples, U and 10 at the lower side of the line, can be drawn. As an example, Fig. 30 is a flow vector diagram showing the state of flow separation in the verification example of U.

[0079] It was confirmed by the inventors of the present invention that the flow separation emerges in the aft part from the location of non-dimensional meridional distance $m=0.4$ to the impeller exit ($m=1.0$) when $MS-s$ is lower than the lower limit of $MS-s_{LIM}$, but there exists another lower limit in the fore part of the blade toward the impeller inlet ($m=0$) different from the lower limit of the Mach number slope at the shroud side $MS-s_{LIM}$ in the aft part from the location of non-dimensional meridional distance $m=0.4$. In order to prevent flow separation caused by the steep Mach number slope at the shroud side in the fore part of the location toward the impeller inlet ($m=0$), the location of non-dimensional meridional distance m at which the minimum value ΔC_{pm} of the reduced static pressure difference ΔC_p emerges is preferably selected to be in the range of non-dimensional meridional distance $m=0.8-1.0$, i.e. in the aft part toward the impeller exit ($m=1.0$).

[0080] Referring back to Fig. 7(A), in the lower part of Fig. 7(A), concerning compressor of a specific speed $N_s=488$, values of the Mach number slope at the shroud side $MS-s$ and the Mach number slope at the hub side $MS-h$, as can be referenced in Fig. 25, were read from the Mach number curves of the verification examples shown in Figs. 24 through 29 in the order of P, Q, R, S, T and U, and shown. In each of verification examples, the calculation process of MSF-angle, the criterion of judgement by MSF-angle and the evaluation process for evaluating the secondary flow suppression quantitatively are the same as the description related to Fig. 4, thus further explanation may be omitted.

[0081] In the present invention, the verification examples in Fig. 4 for pumps are presented in the range of the specific speed $N_s=280-560$. According to the concept of the present invention, there will be another optimum value for the range of the specific speed of not more than $N_s=280$. However, as is observed from the tendency of the inclined boundary lines in Fig. 4, the D_{280} value is lower than D_{400} and D_{560} value, and D_{400} value is lower than D_{560} value. So, the critical value of D has a tendency to have lower value for an impeller having a lower specific speed, although the quantitative dependency on the specific speed is not clear in Fig. 4 (the quantitative dependency is clarified in the following second aspect of the present invention). Therefore, the impeller, having suppressed meridional secondary

flow, can be designed in safety by using D value of not less than $D_{280}=0.2$ for the specific speed range of not more than $N_s=280$. Similarly, the impellers, having suppressed meridional secondary flows, for the specific speed range of not more than $N_s=400$ and $N_s=560$ can be designed in safety by using D value of not less than $D_{400}=0.28$ and $D_{560}=0.35$, respectively.

5 **[0082]** In the compressor, only the data of the specific speed of $N_s=488$ are presented in Fig. 5. However, the flow mechanism leading to the suppression of the meridional secondary flows is the same between pumps and compressors, and so the compressor impellers, having suppressed meridional secondary flow, for the specific speed range of not more than $N_s=488$ can be designed in safety by using DM value of not less than $DM_{488}=0.23$.

[0083] Next, an embodiment according to the second aspect of the present invention will be described below.

10 **[0084]** According to the embodiment of the first aspect of the present invention, the boundary lines of the inclined straight lines are confirmed and drawn in Fig. 4 or Fig. 5 dispersively for each of the specific speeds of the turbomachinery or sorts of fluid (incompressible fluid or compressible fluid), and the dependence of data on the specific speed is not made evident quantitatively. Therefore, concerning the turbomachinery having a certain specific speed and handling a certain kind of fluid, when designing suitably the contribution in the pressure coefficient slope at the shroud side CPS-s and the pressure coefficient slope at the hub side CPS-h or the Mach number slope at the shroud side MS-s and the Mach number slope at the hub side MS-h from the aspect of secondary flow suppression so that the difference D between a minimum value ΔC_{pm} of the reduced static pressure difference ΔC_p and the value $\Delta C_{p_{m-0.4}}$ of the reduced static pressure difference ΔC_p at the location corresponding to non-dimensional meridional distance mm-0.4 obtained by subtracting non-dimensional meridional distance 0.4 from non-dimensional meridional distance mm representing the minimum value ΔC_{pm} or the difference DM between the minimum value ΔM_m of the relative Mach number difference ΔM and a value $\Delta M_{m-0.4}$ of the relative Mach number difference ΔM at the location corresponding to non-dimensional meridional distance 0.4 from non-dimensional meridional distance representing the minimum value amounts to a certain value or more, there are cases to which the boundary lines shown on the plane of Fig. 4 or Fig. 5 are not directly applicable.

15 **[0085]** Therefore, according to the second aspect of the present invention, with respect to the difference D between a minimum value ΔC_{pm} of the reduced static pressure difference ΔC_p and a value $\Delta C_{p_{m-0.4}}$ of the reduced static pressure difference ΔC_p or the difference DM between a minimum value ΔM_m of the relative Mach number difference ΔM and a value $\Delta M_{m-0.4}$ of the relative Mach number difference ΔM , the dependence on the specific speed is clarified in spite of sorts of fluid. That is, concerning the difference D or DM, the pressure coefficient C_p^* which is normalized by the pressure coefficient $C_{p, \text{mid-mid}}$ in the center of fluid passage is introduced and newly defined, whereby the boundary line according to the first aspect of the present invention can be expressed as a function of the specific speed N_s .

20 **[0086]** Fig. 6 shows the plotted data about the above difference on the basis of the normalized pressure difference C_p^* in verification examples. In Fig. 6, the vertical axis represents the difference D^* between the normalized reduced static pressure difference $\Delta C_{p_{m-0.4}}^*$ at the location of non-dimensional meridional distance mm-0.4 and a minimum value $\Delta C_{p_m}^*$ the normalized reduced static pressure difference ΔC_p^* at the location of non-dimensional meridional distance mm, and the horizontal axis represents a specific speed N_s of the turbomachinery. Data plotted on the plane defined by both axes are the same as the data plotted on the plane of Figs. 4 and 5. A boundary line of an negatively sloped straight line can be drawn so that data shown by open symbols representing adaptation to the quantitative criterion of judgement about suppression of the secondary flow are located on the data area at the upper right of the drawing, and data shown by solid symbols representing nonadaptation to the quantitative criterion of judgement about suppression of the secondary flow are located on the data area at the lower left of the drawing.

25 **[0087]** By reading the gradient of the boundary line, and the intersection of the boundary line and the vertical axis, as a function which is dependent on the specific speed N_s and represents the difference D^* of the normalized reduced static pressure difference, the appropriateness of the following equation was confirmed.

$$D^* = \Delta C_{p_{m-0.4}}^* - \Delta C_{p_m}^* = -0.004 N_s + 3.62$$

30 where the normalized pressure coefficient is defined in the following equation.

$$C_p^* = C_p / C_{p, \text{mid-mid}}$$

35 where $C_{p, \text{mid-mid}}$ is a pressure coefficient in the center of the flow channel as shown in Fig. 1(D).

[0088] In compressors which handle compressive fluid, the relative Mach number M can be related to the pressure coefficient C_p by the following equation, thus the normalized pressure coefficient C_p^* is applicable to every kinds of fluid.

$$C_p = 2[1 - (1 - 0.5W^2/H_0^*)^{\gamma/(\gamma-1)}] / \gamma M_0^{*2}$$

$$M_0^* = Ut / (\gamma P_0^* / \rho_0^*)^{0.5}$$

where Ut is a peripheral speed of the impeller, W is a relative velocity, H_0^* is a rothalpy, γ is a ratio of specific heats, P_0^* is a rotary stagnation pressure, and ρ_0^* is a density corresponding to P_0^* .

[0089] In verification examples, the differences ($D^* = \Delta C_p^*_{m-0.4} - \Delta C_p^*_{m-0.4}$) of the reduced static pressure differences, which are basis of the values of the data plotted on the plain of FIG. 6, are shown in a table of FIG. 7(B).

[0090] Incidentally, verification examples 7 and 8 are related to the pumps of a specific speed $N_s=377$. It was confirmed that the data of the above verification examples are defined by the boundary line on the plane of FIG. 6, and located on the data area of nonadaptation to suppression of the secondary flow. Incidentally, it is confirmed by the three-dimensional viscous calculations that the value of pressure coefficient slope at the shroud side which is negative and extremely small (steep), compared with the lower limit of the pressure coefficient slope at the shroud side $CPS_{s,LIM}$, emerges in the fore part toward the impeller inlet ($m=0$) from the location of non-dimensional meridional distance $m-0.4$, therefore flow separation is generated in the fore part of the impeller. Therefore, the information on the secondary flow development in the verification data of 7 and 8 could not be ascertained.

[0091] An embodiment according to the third and fourth aspects of the present invention will be described below. When designing and manufacturing a turbomachinery having an impeller with three-dimensional shape for realizing the remarkably decreasing tendency in the reduced static pressure difference ΔC_p or the relative Mach number difference ΔM characterized by the first aspect of the present invention along the location of non-dimensional meridional distance m toward the impeller exit in the third aspect of the present invention, and when designing and manufacturing a turbomachinery having an impeller with three-dimensional shape for realizing the remarkably decreasing tendency in the reduced static pressure difference ΔC_p^* characterized by the second aspect of the present invention on the basis of the normalized pressure coefficient C_p^* , the following design method for the three-dimensional geometry of the impeller is utilized. The design method comprises a first step of determining the meridional geometry, a second step of determining the blade loading distribution, a third step of determining blade profile, a fourth step of judging the optimum reduced static pressure difference ΔC_p and the like, and a fifth step of evaluating flow fields.

[0092] In these aspects, while selecting properly by trial and error the blade loading distribution on the basis of the known close relationship between the pressure coefficient C_p and the angular momentum $r\bar{V}_\theta$, the pressure coefficient C_p is increased or decreased. And, by utilizing the following three-dimensional inverse design method using the $r\bar{V}_\theta$ distribution as an input data, the three-dimensional shape of the impeller which realize a characteristic distribution characterized by the first and second aspects of the present invention is determined.

[0093] In this case, the design method is processed by the flow chart shown in Fig. 3(B).

[0094] In the first step (step of determining meridional geometry), based on the conventional knowledge about the correlation with the specific speed N_s calculated from the design specification, the meridional shape of hub and the shroud and the position of the leading edge of the blade and the trailing edge of the blade are defined, and the number of blades of the impeller is selected. Mesh required for numerical calculation is formed at an equal interval or unequal interval along the hub and the shroud surfaces. This mesh is extended to the upstream of the leading edge of the blade and the downstream of the trailing edge of the blade. The mesh is similar to that in Fig. 1(C) of the mesh for viscous flow calculations. Quasi-Orthogonal line (Q-O line) is drawn by connecting the corresponding points on the hub and the shroud. Next, a plurality of surfaces of revolution is defined in the meridional flow channel, and the stacking condition f_0 (tangential co-ordinate of the blade camber line at a point on each of surfaces of revolution). The process in the first step is essentially the same as the process in the first step of the conventional design method shown in Fig. 3(A).

[0095] In the second step (step of determining blade loading distribution), the shape of the blade loading distribution $\partial(r\bar{V}_\theta)/\partial m$ is selected so that the blade loading distribution has a peak on the shroud surface in the first half of the non-dimensional meridional distance m along the shroud and a peak on the hub surface in the latter half of the non-dimensional meridional distance m along the hub. Next, the distribution of $\partial(r\bar{V}_\theta)/\partial m$ along the hub and shroud is integrated along the non-dimensional meridional distance m to determine $r\bar{V}_\theta$ distribution. The resultant value on the hub and the shroud surfaces obtained by integration along the non-dimensional meridional distance m is adjusted to satisfy the exit velocity triangles (i.e. the \bar{V}_θ values on the hub and the shroud at the impeller exit determined, in the similar manner as the conventional method, from the design head of the impeller), and the $r\bar{V}_\theta$ distribution between the hub and the shroud is determined by the linear interpolation along Q-O line determined by the first step.

[0096] In the third step (step of determining blade profile), the blade camber line is obtained by applying the condition that the velocity is along the blade at the blade camber line, i.e. there is no flow through the blade camber.

[0097] If we represent the location of the blade camber line α , which is defined as:

EP 0 865 577 B1

$$\alpha = \theta - f(r, z) = 0, n2\pi/B, (n = 1, 2, 3 \dots B)$$

where f is the tangential co-ordinate of the blade camber line (or wrap angle), θ is the tangential co-ordinate of cylindrical polar co-ordinate system, and B is the number of blades (as shown in Fig. 1(E)).

[0098] The above condition is expressed mathematically in the following equation.

$$W_+ \cdot \nabla(\alpha) = 0, W_- \cdot \nabla(\alpha) = 0$$

where W_+ and W_- are the relative velocity of the pressure and the suction surfaces of the blade, respectively, ∇ is vector calculus operator.

[0099] The above two equations are combined to give the following equation.

$$W_{b1} \cdot \nabla \alpha = 0 \quad \text{where } W_{b1} = (W_+ + W_-)/2$$

[0100] The above equation can be decomposed into its components and expressed in the following equation.

$$\begin{aligned} & \{(\bar{V}z + v_{zb1})\partial f/\partial z\} + \{(\bar{V}r + v_{rb1})\partial f/\partial r\} \\ & = \{(r\bar{V}_\theta)/r^2\} + \{(v_{\theta b1})/r\} - \omega \end{aligned}$$

[0101] The above equation is a first order hyperbolic partial differential equation. The value of f_0 along an arbitrary Q-O line in the blade (the stacking condition) is used as initial value, and the above equation is integrated along the non-dimensional meridional distance m, and the tangential co-ordinate of the blade camber line f in the location of non-dimensional meridional distance m is determined. And, the three-dimensional geometry of the impeller is determined by adding a certain thickness to the determined blade camber line to allow the blade to have required mechanical strength. The stacking condition can be specified by, for example, setting the zero value of f_0 along the Q-O line at the blade trailing edge, or setting a moderate distribution of f_0 value along the Q-O line at the blade trailing edge.

[0102] The calculation of the relative velocity W, appeared in the above mentioned equations, is processed in the following manner.

[0103] The velocity field is split into a tangentially-averaged and tangentially periodic components. To determine the tangentially-averaged flow the radial and axial velocities ($\bar{V}r$ and $\bar{V}z$, respectively) are expressed in terms of a stream function in order to satisfy the continuity (or mass conservation) equation of fluid dynamics. Then a Poisson type partial differential equation governing the streamfunction is obtained by using a suitable equation for the vorticity field generated by the action of the blades, which in turn is related to the blade circulation $2\pi r\bar{V}_\theta$. This equation can then be integrated by any suitable numerical method subject to uniform velocity condition at upstream and downstream boundaries and no flow (or constant stream function) conditions at the hub and shroud walls. Integration of this equation will give the values of streamfunction from which $\bar{V}r$ and $\bar{V}z$ are obtained.

[0104] The velocity terms v_{rb1} , v_{zb1} and $v_{\theta b1}$ are obtained from the solution of the tangentially periodic flow. For the solution of the periodic flow the Clebsch formulation of the velocity field is used. In this formulation the velocity field is split into an unknown irrotational part (represented by a velocity potential function) and a known rotational part which is related to the blade circulation $2\pi r\bar{V}_\theta$. The governing equation of the unknown potential function is then found by using Clebsch formulation for the velocity field in the continuity equation of the periodic flow. In this way a 3D Poisson's equation is obtained which can then be integrated by a suitable numerical technique, subject to vanishing periodic tangential velocity and spanwise velocity at upstream and downstream boundaries and no-flow conditions through the hub and shroud surface.

[0105] According to the above method, velocity field as well as blade loading of the impeller, i.e. the pressure difference $p(+)$ - $p(-)$ between the pressure $p(+)$ on pressure surface and the pressure $p(-)$ on the suction surface of the blade can be obtained in the following equation.

$$\{p(+)-p(-)\}/\rho = 2\pi(W_{b1} \cdot \nabla r \bar{V}_\theta)/B,$$

where W_{b1} is relative velocity at the location on blade surface.

[0106] In this way, the reduced static pressure difference ΔCp or the relative Mach number difference ΔM between

the hub and the shroud on the suction surface of the blade can be obtained.

[0107] Further, the value which is not dependent on the specific speed and the type of the impeller, i.e. both for the compressor which handles compressible fluid and the pump which handles incompressible fluid, the normalized pressure coefficient Cp^* is defined as follows.

$$Cp^* = Cp/Cp_{,mid-mid}$$

where $Cp_{,mid-mid}$ is the pressure coefficient at the center of the flow channel (midspan and midpitch) at the location of non-dimensional meridional distance m . The pressure coefficient Cp in compressible fluid is defined in the following equation.

$$Cp^* = 2[1-(1-0.5W^2/H_0^*)^{\gamma/(\gamma-1)}]/\gamma M_0^{*2}$$

$$M_0^{*2} = Ut/(\gamma P_0^*/\rho_0^*)^{0.5}$$

where Ut is a peripheral speed of the impeller, W is a relative velocity, H_0^* is a rothalpy, γ is a ratio of specific heats, P_0^* is a rotary stagnation pressure, and ρ_0^* is a density corresponding to P_0^* .

[0108] In the fourth step (a step of judging optimum reduced static pressure difference ΔCp and the like), it is judged whether or not the distribution of the reduced static pressure difference ΔCp or the relative Mach number difference ΔM along the location of non-dimensional meridional distance m calculated in the third step is suitable for suppression of the secondary flow in the impeller. When establishing the distribution of reduced static pressure difference ΔCp for realizing suppression of the secondary flow, the decreasing tendency in the reduced static pressure difference ΔCp is realized by (a) the degree of dependence on a variation at the shroud side, (b) the degree of dependence on a variation at the hub side, and (c) the degree of dependence on both variation at the shroud side and the hub side. In order to judge the suitable ΔCp distribution numerically, the pressure coefficient slope on the suction surface of the blade at the shroud side $CPS-s$ and the pressure coefficient slope on the suction surface of the blade at the hub side $CPS-h$ between the location of a minimum value ΔCp_m of the reduced static pressure difference ΔCp and the location of non-dimensional meridional distance $mm-0.4$ obtained by subtracting non-dimensional meridional distance 0.4 from non-dimensional meridional distance mm representing the minimum value ΔCp_m are defined, and it is judged whether this value satisfies the criteria defined in the first aspect of the present invention. In the case where the variation of ΔCp is largely dependent on the variation of the shroud side, and the pressure distribution becomes such that excessive pressure increase (or excessive deceleration of the relative velocity) occurs, a great amount of flow separation is occurred at the same area generating lower head, poor efficiency or decrease in operational range. Therefore, care should be taken so as not to cause such distribution based on the $CPS-s_{,LIM}$ limit defined in the first aspect of the present invention.

[0109] Incidentally, in case of incompressible fluid, the pressure coefficient Cp is equal to $(W/U)^2$, where W is relative velocity. In compressible fluid as in compressors, the physical variable related to the behavior of secondary flow is relative Mach number. Therefore, in case of compressible fluid, the same judgement concerning the reduced static pressure difference ΔCp is applied to the relative Mach number difference ΔM based on the criteria defined in the first aspect of the present invention.

[0110] Further, by using the normalized pressure coefficient Cp^* proposed for design criterion of secondary flow suppression as common design criterion concerning pumps and compressors, it is possible to judge from the difference between a minimum value ΔCp^*_m of the normalized reduced static pressure difference ΔCp^* and a value $\Delta Cp^*_{m-0.4}$ of the normalized reduced static pressure difference ΔCp^* at the location corresponding to non-dimensional meridional distance $mm-0.4$ obtained by subtracting non-dimensional meridional distance 0.4 from non-dimensional meridional distance mm representing the minimum value ΔCp_m .

[0111] By the above manner, it is judged whether the optimum reduced static pressure difference can be obtained, if it is not satisfied, after going back to the second step to modify the blade loading distribution, the steps from the second step to the above steps are repeated until the optimum reduced static pressure difference is obtained. After completing this step, the blade loading distribution $\partial(r\bar{V}_\theta)/\partial m$ in which optimum reduced pressure distribution can be obtained is determined. As a result, in the design of an impeller having similar design specification, above mentioned optimum distribution of the blade loading $\partial(r\bar{V}_\theta)/\partial m$ is applicable, and the optimization process for the new design can be greatly accelerated.

[0112] In the fifth step (step of evaluation of flow fields), a possibility of poor performance caused by the flow separation due to rapid deceleration or rapid pressure increase in the impeller determined by the third step is evaluated. In

the case

where it is judged that the pressure distribution in the impeller is not appropriate, after going back to the second step to modify the blade loading distribution, the steps from the second step to the fifth step are repeated until the expected result is achieved.

5 [0113] In the second step of the third and fourth aspects of the present invention, the characteristics of flow fields, i.e. the blade loading distribution directly related to the flow physics, is used as input data for the third step to determine the blade profile, therefore the blade profile for suppressing the secondary flow can be promptly designed and the impeller having such blade profile can be easily manufactured, compared with the conventional manufacturing method using the modification of blade angle distribution by trial and error.

10 [0114] Incidentally, concerning the method in the third step to obtain the blade profile based on the specified $r\bar{V}_\theta$ distribution determined in the second step, another inverse design methods including the effects of the finite blade thickness on the velocity fields or semi-inverse method such as Soulis, J.V., 1985, "Thin Turbomachinery Blade Design Using A Finite-Volume Method", International Journal of Numerical Methods in Engineering, vol.21, p.19, which based on iterative application of analysis methods, are available. However, these methods require more computational time and are less efficient compared with that described in the third step of the third and fourth aspect of the present invention.

Industrial Applicability

20 [0115] According to the present invention, there is provided a turbomachinery having an impeller, characterized in that the impeller is designed so that the reduced static pressure difference ΔC_p or the relative Mach number difference ΔM between the hub and the shroud on the suction surface of a blade shows a remarkably decreasing tendency along the location of non-dimensional meridional distance m toward the impeller exit.

25 (1) In order to obtain the above remarkably decreasing tendency, the blade profile of the impeller is determined by utilizing the three-dimensional inverse design method using the blade loading distribution as input data so that the difference D between a minimum value ΔC_{p_m} of the reduced static pressure difference ΔC_p and a value $\Delta C_{p_{m-0.4}}$ of the reduced static pressure difference ΔC_p at the location corresponding to non-dimensional meridional distance $m-0.4$ obtained by subtracting non-dimensional meridional distance 0.4 from non-dimensional meridional distance m representing the above minimum value ΔC_{p_m} is selected to be a specified value which is dependent on a specific speed of the turbomachinery. Further, the difference DM between a minimum value ΔM_m of the relative Mach number difference ΔM and a value $\Delta M_{m-0.4}$ of the relative Mach number difference ΔM at the location corresponding to the above non-dimensional meridional distance $m-0.4$ is also selected to be a specified value which is dependent on a specific speed of the turbomachinery.

30 (2) Instead of the pressure coefficient C_p or the Mach number M , and thus the reduced static pressure difference ΔC_p or the relative Mach number difference ΔM , the normalized pressure coefficient C_p^* is commonly used for compressible fluid and incompressible fluid so that the normalized pressure coefficient difference D^* corresponding to the above difference D or DM is expressed as a function of the specific speed N_s . Then, the blade profile of the impeller is determined by utilizing the three-dimensional inverse design method using the blade loading distribution as input data so that the above difference D^* corresponding to the turbomachinery of a given specific speed is selected to be a specified value which complies with the above function.

35 (3) The turbomachinery is designed and manufactured by utilizing the three-dimensional inverse design method using the aspects characterized by the above (1) and (2) as input data.

40 [0116] With regard to the above-described aspects (1)-(3), those propriety is substantiated by a large amount of verification data, therefore the present invention can be utilized effectively in industry.

45 [0117] According to the above aspects, since the meridional component of secondary flow can be effectively suppressed, a loss which occurs in the turbomachinery or the down stream flow channel can be reduced, emergence of positively sloped characteristic curve can be avoided, and stability of operation can be improved. Therefore, the present invention has a great utility value in industry.

Claims

50 1. A turbo machine having an impeller with a plurality of blades supported by a hub on which said blades are circumferentially spaced and covered by a shroud surface which forms an outer boundary to flow of fluid in a flow passage defining a flow direction between two adjacent blades, **characterized in that:**

said impeller has a configuration such that one of a reduced static pressure difference ΔC_p and a relative Mach number difference ΔM between the hub and the shroud on the suction surface of the blade shows a remark-

ably decreasing tendency along the location of non-dimensional meridional distance in toward the impeller exit and is selected to be not less than a specified value which is dependent on a specific speed N_s of the turbomachines, herein specific speed N_s is defined as $N_s = NQ^{0.5}/H^{0.75}$, where N is the rotational speed in revolutions per minute, Q is the flow rate at an impeller inlet in cubic meters per minute, and H is the head in meters representing fluid energy which is imparted to the fluid by the turbomachine;

said remarkably decreasing tendency of ΔC_p for the turbomachine handling incompressible fluid is arranged such that the reduced static pressure difference between a minimum value ΔC_{pm} of reduced static pressure difference ΔC_p and a value $\Delta C_{pm-m-0.4}$ of reduced static pressure difference ΔC_p at the location corresponding to non-dimensional meridional distance $m_{m-0.4}$ obtained by subtracting non-dimensional meridional distance 0.4 from non-dimensional meridional distance m_m representing said minimum value ΔC_{pm} is selected to be not less than 0.20 at said specific speed N_s of not more than 280, not less than 0.28 at said specific speed N_s of not more than 400, and not less than 0.35 at said specific speed N_s of not more than 560; and

said remarkably decreasing tendency of ΔM for the turbomachine handling compressible fluid is arranged such that relative Mach number difference between minimum value ΔM_m of the relative Mach number difference ΔM and a value $\Delta M_{m-0.4}$ of the relative Mach number difference ΔM at the location corresponding to non-dimensional meridional distance $M_{m-0.4}$ obtained by subtracting non-dimensional meridional distance 0.4 from non-dimensional meridional distance M_2 representing said minimum value ΔM_m is selected to be not less than 0.23 at said specific speed of not more than 488.

2. The turbomachine as recited in claim 1, wherein the non-dimensional meridional distance M_m representing said minimum value ΔC_{pm} of the reduced static pressure difference ΔC_p is selected to be in the range of non-dimensional meridional distance $m=0-8.0$.

3. The turbomachine as recited in claim 1 or claim 2, wherein a pressure coefficient slope at the shroud side $CPS-s$ on the suction surface of the blade is selected to be not less than -1.3 as a lower limit of the pressure coefficient slope at the shroud side $CPS-s_{LIM}$.

4. The turbomachine as recited in claim 1, wherein a Mach number slope at the shroud side $MS-s$ on the suction surface of the blade is selected to be not less than -0.8 as a lower limit of the Mach number slope at the shroud side $MS-s_{LIM}$.

5. The turbomachine as recited in claim 1 or claim 4, wherein the non-dimensional meridional distance M_2 representing said minimum value ΔM of the relative Mach number difference ΔM is selected to be in the range of non-dimensional meridional distance $m=0.8-1.0$.

6. A method of manufacturing a turbomachine having an impeller with a plurality of blades supported by a hub on which said blades are circumferentially spaced and covered by a shroud surface which forms an outer boundary to flow of fluid in a flow passage defining a flow direction. between two adjacent blades, comprising:

a first step of selecting meridional geometry and the number of blades of the impeller using design specification as input data, defining a plurality of surface of revolution in a meridional flow channel, and determining stacking condition f_0 ;

a second step of determining distribution of blade loading rV_θ along non-dimensional meridional distance m by selecting a shape of the blade loading distribution $\delta(rV_\theta)/\delta m$ which has a peak on the shroud surface in the first half of the location of non-meridional distance m and a peak on the hub surface in the latter half of the location of non-dimensional meridional distance, adjusting a value obtained by integrating the blade loading distribution along the non-dimensional meridional distance m so as to satisfy design head of the impeller;

a third step of determining three-dimensional geometry of the impeller by integrating

$$\{(\bar{V} z + v_{zb1})\delta f/\delta z\} + \{(\bar{V} r + v_{rb1})\delta f/\delta r\} = \{(r\bar{V}_\theta)/r^2\} + \{(v_{ob1})/r\} - \omega$$

along non-dimensional meridional distance m using stacking condition f_0 as initial value to determine tangential co-ordinate f of the blade camber line in non-dimensional meridional distance m and adding a certain thickness to the determined value to allow the blade to have required mechanical strength;

a fourth step of judging whether one of the distribution of reduced static pressure difference ΔC_p and the distribution of a relative Mach number difference ΔM along non-dimensional meridional distance m obtained

by the third step is suitable for suppressing the secondary flow in the impeller or not;
 a fifth step of evaluating possibility of poor performance caused by at least flow separation in the impeller
 determined by the third step, evaluating secondary flow in the impeller by a secondary flow parameter, and
 after going back to the second step to modify the blade loading distribution on the basis of the above evaluation,
 repeating the above steps until the expected result is achieved;

wherein one of a reduced static pressure difference ΔC_p and a relative Mach number difference ΔM between
 the hub and the shroud on the suction surface of the blade shows a remarkably decreasing tendency along the
 location of non-dimensional meridional distance m toward the impeller exit and is selected to be not less than a
 specified value which is dependent on a specific speed N_s of the turbomachines, herein specific speed N_s is
 defined as $N_s = NQ^{0.5}/H^{0.75}$, where N is the rotational speed in revolution per minutes, Q is the flow rate at an
 impeller inlet in cubic meter per minutes, and H is the head in meter representing fluid energy which is imparted
 to the fluid by the turbomachine;

said remarkably decreasing tendency of ΔC_p for the turbomachine handling incompressible fluid is arrange
 such that the reduced static pressure difference between a minimum value ΔC_{pm} of reduced static pressure dif-
 ference ΔC_p and a value $\Delta C_{pm-0.4}$ of reduced static pressure difference ΔC_p at the location corresponding to non-
 dimensional meridional distance $m_{m-0.4}$ obtained by subtracting non-dimensional meridional distance 0.4 from non-
 dimensional meridional distance m_m representing said minimum value ΔC_{pm} is selected to be

not less than 0.20 at said specific speed N_s of not more than 280,
 not less than 0.28 at said specific speed N_s of not more than 400, and
 not less than 0.35 at said specific speed N_s of not more than 560; and

said remarkably decreasing tendency of ΔM for the turbomachine handling compressible fluid is arranged
 such that relative Mach difference between a minimum value ΔM_m of the relative Mach number difference ΔM and
 a value $\Delta M_{m-0.4}$ of the relative Mach number difference ΔM at the location corresponding to non-dimensional me-
 ridional distance $m_{m-0.4}$ obtained by subtracting non-dimensional meridional distance 0.4 from non-dimensional
 meridional distance m_m representing said minimum value ΔM_m is selected to be not less than 0.23 at said specific
 speed of not more than 488.

7. The method of manufacturing the turbomachine as recited in claim 6, wherein it is judged whether the non-dimen-
 sional meridional distance m_m representing said minimum value ΔC_{pm} of the reduced static pressure difference
 ΔC_p is in the range of non-dimensional meridional distance $m=0.8-1$ or not.

8. The method of manufacturing the turbomachine as recited in claim 6 or 7, wherein it is judged whether pressure
 coefficient slope at the shroud side CPS-s on the suction surface of the blade is not less than -1.3 as a lower limit
 of the pressure coefficient slope at the shroud side CPS-s_{LIM}.

9. The method of manufacturing the turbomachine as recited in claim 6, wherein it is judged whether the Mach number
 slope at the shroud side MS-s on the suction surface of the blade is not less than -0.8 as a lower limit of the Mach
 number slope at the shroud side MS-s_{LIM}.

10. The method of manufacturing the turbomachine as recited in claim 6 or 9, wherein it is judged whether the non-
 dimensional meridional distance m_m representing said minimum value ΔM_m of the relative Mach number difference
 ΔM is in the range of non-dimensional meridional distance $m=0.8-1.0$.

Patentansprüche

1. Eine Turbomaschine mit einem Laufrad mit einer Vielzahl von Schaufeln, die auf einer Nabe getragen sind, auf
 der die Schaufeln umfangsmäßig voneinander beabstandet sind und von einer Umhüllungsfläche abgedeckt
 sind, die eine äußere Begrenzung für die Strömung eines Strömungsmittels in einem Strömungsdurchlass bildet,
 der eine Strömungsrichtung zwischen zwei benachbarten Schaufeln definiert, **dadurch gekennzeichnet, dass:**

das Laufrad eine Konfiguration aufweist, so dass eines von beidem einem reduzierten statischen Druckunter-
 schied ΔC_p und einem relativen Machzahlunterschied ΔM zwischen der Nabe und der Umhüllung auf der
 Saugoberfläche der Schaufel eine deutlich abfallende Tendenz entlang des Ortes eines dimensionslosen Me-
 ridionalabstandes m in Richtung auf den Laufradausgang zeigt und auf nicht weniger als ein spezifizierter
 Wert ausgewählt ist, der von einer spezifischen Geschwindigkeit N_s der Turbomaschinenen abhängt, wobei
 hier die spezifische Geschwindigkeit N_s definiert ist als $N_s = NQ^{0.5}/H^{0.75}$, wobei N die Drehgeschwindigkeit in

Umdrehungen pro Minute ist, Q die Strömungsrate am Laufradeinlass in Kubikmeter pro Minute, und H der Hub in Metern ist, was die Strömungsmittelenergie repräsentiert, die dem Strömungsmittel durch die Turbomaschine erteilt wird;

wobei die deutlich abfallende Tendenz von ΔC_p für die Turbomaschine, die ein nicht verdichtbares Fluid handhabt, derart ausgelegt ist, dass der reduzierte statische Druckunterschied zwischen einem Minimalwert ΔC_{pm} des reduzierten statischen Druckunterschied ΔC_p und einem Wert $\Delta C_{pm-0,4}$ des reduzierten statischen Druckunterschieds ΔC_p an dem Ort entsprechend dem dimensionslosen Meridionalabstand $m_{m-0,4}$ erhalten durch die Subtraktion eines dimensionslosen Meridionalabstandes 0,4 vom dimensionslosen Meridionalabstand m_m , der den Minimalwert ΔC_{pm} repräsentiert, ausgewählt ist zu:

nicht weniger als 0,20 bei der spezifischen Geschwindigkeit N_s von nicht mehr als 280, nicht weniger als 0,28 bei der spezifischen Geschwindigkeit von nicht mehr als 400, und nicht weniger als 0,35 bei der spezifischen Geschwindigkeit von nicht mehr als 560; und

wobei die deutlich abnehmende Tendenz von ΔM für die Turbomaschine, die ein verdichtbares Strömungsmittel handhabt, derart ausgelegt ist, dass der relative Machzahlunterschied zwischen einem Minimalwert ΔM_m des relativen Machzahlunterschieds ΔM und einem Wert $\Delta M_{m-0,4}$ des relativen Machzahlunterschieds ΔM an dem Ort, der dem dimensionslosen Meridionalabstand $M_{m-0,4}$ entspricht, der erhalten wird durch Subtraktion eines dimensionslosen Meridionalabstandes 0,4 vom dimensionslosen Meridionalabstand M_2 , der den Minimalwert ΔM_m repräsentiert, ausgewählt ist auf nicht weniger als 0,23 bei der spezifischen Geschwindigkeit von nicht mehr als 488.

2. Turbomaschine nach Anspruch 1, wobei der dimensionslose Meridionalabstand M_m , der den Minimalwert ΔC_{pm} des reduzierten statischen Druckunterschiedes ΔC_p repräsentiert, ausgewählt ist, so dass er in einem Bereich von einem dimensionslosen Meridionalabstand $m=0-8,0$ liegt.
3. Turbomaschine nach Anspruch 1 oder nach Anspruch 2, wobei eine Druckunterschiedsteigung an der Seite der Umhüllung CPS-s auf der Saugoberfläche der Schaufel ausgewählt ist, so dass sie nicht kleiner ist als -1,3 als eine untere Grenze der Druckunterschiedsteigung an der Seite der Umhüllung CPS-s_{LIM}.
4. Turbomaschine nach Anspruch 1, wobei eine Machzahlsteigung an der Seite der Umhüllung MS-s auf der Saugoberfläche der Schaufel ausgewählt ist, so dass sie nicht kleiner ist als -0,8 als eine untere Grenze der Machzahlsteigung an der Seite der Umhüllung MS-s_{LIM}.
5. Turbomaschine nach Anspruch 1 oder Anspruch 4, wobei der dimensionslose Meridionalabstand M_2 , der den Minimalwert ΔM des relativen Machzahlunterschieds ΔM repräsentiert, ausgewählt ist, so dass er in einem Bereich des dimensionslosen Meridionalabstandes $m=0,8-1,0$ liegt.
6. Verfahren zur Herstellung einer Turbomaschine mit einem Laufrad mit einer Vielzahl von Schaufeln, die durch eine Nabe getragen sind, auf der die Schaufeln umfangsmäßig voneinander beabstandet sind und von einer Umhüllungsoberfläche abgedeckt sind, die eine äußere Begrenzung für die Strömung von Strömungsmittel in einem Strömungsmitteldurchlass bildet, der eine Strömungsrichtung definiert zwischen benachbarten Schaufeln, wobei das Verfahren folgendes aufweist:

einen ersten Schritt des Auswählens einer meridionalen Geometrie und der Anzahl von Schaufeln des Laufrades unter Nutzung einer Konstruktionspezifikation als Eingabedaten, Definieren einer Vielzahl von Umdrehungsoberflächen in einem meridionalen Strömungskanal, und Bestimmen des Stapel- bzw. Aufschichtungszustandes f_0 ;

einen zweiten Schritt des Bestimmens der Verteilung der Schaufellast rV_θ entlang eines dimensionslosen Meridionalabstandes m durch Auswählen einer Form der Schaufellastverteilung $\delta(rV_\theta)/\delta m$, die eine Spitze auf der Umhüllungsoberfläche in der ersten Hälfte des Ortes des dimensionslosen Meridionalabstandes m und eine Spitze auf der Nabenoberfläche in der letzteren Hälfte des Ortes des dimensionslosen Meridionalabstandes hat, Einstellen eines Wertes erhalten durch Integrieren der Schaufellastverteilung entlang des dimensionslosen Meridionalabstandes m , so dass der Konstruktionshub des Laufrades erfüllt wird;

einen dritten Schritt des Bestimmens einer dreidimensionalen Geometrie des Laufrades durch Integrieren von

$$\{(\bar{V}_z + v_{zb1})\delta f / \delta z\} + \{(\bar{V}_r + v_{rb1})\delta f / \delta r\} = \{(r\bar{V}_\theta) / r^2\} + \{(V_{ob1}) / r\} - \bar{\omega}$$

entlang dem dimensionslosen Meridionalabstand m unter Verwendung des Stapel- bzw. Aufschichtungszustandes f_0 als Anfangswert zum Bestimmen einer Tangentialkoordinate f der Schaufelwölbungsline in dimensionslosem Meridionalabstand m und Addieren einer bestimmten Dicke zum bestimmten Wert, um zu gestalten, dass die Schaufel eine erforderliche mechanische Stärke hat;

eine vierte Schritt des Beurteilens, ob eines der beiden der Verteilung des reduzierten statischen Druckunterschiedes ΔC_p und der Verteilung eines relativen Machzahlunterschieds ΔM entlang des dimensionslosen Meridionalabstandes m erhalten im dritten Schritt geeignet ist für die Unterdrückung der Sekundärströmung im Laufrad oder nicht;

einen fünften Schritt des Auswertens der Möglichkeit einer schlechten Leistung hervorgerufen durch zumindest eine Strömungstrennung im Laufrad bestimmt durch den dritten Schritt, Auswerten einer Sekundärströmung im Laufrad durch einen Sekundärströmungsparameter, und danach Zurückgehen zum zweiten Schritt zum Modifizieren der Schaufellastverteilung auf der Basis der zuvor erwähnten Auswertung, Wiederholen der zuvor genannten Schritte bis das erwartete Resultat erreicht ist;

wobei eines von beidem einem reduzierten statischen Druckunterschied ΔC_p und einem relativen Machzahlunterschied ΔM zwischen der Nabe und der Umhüllung auf der Saugoberfläche der Schaufel eine deutlich abfallende Tendenz entlang des Ortes eines dimensionslosen Meridionalabstandes m in Richtung auf den Laufradausgang zeigt und auf nicht weniger als ein spezifizierter Wert ausgewählt ist, der von einer spezifischen Geschwindigkeit N_s der Turbomaschinen abhängt, wobei hier die spezifische Geschwindigkeit N_s definiert ist als $N_s = NQ^{0,5} / H^{0,75}$, wobei N die Drehgeschwindigkeit in Umdrehungen pro Minute ist, Q die Strömungsrate am Laufradeinlass in Kubikmeter pro Minute, und H der Hub in Metern ist, was die Strömungsmittelenergie repräsentiert, die dem Strömungsmittel durch die Turbomaschine erteilt wird;

wobei die deutlich abfallende Tendenz von ΔC_p für die Turbomaschine, die ein nicht verdichtbares Fluid handhabt, derart ausgelegt ist, dass der reduzierte statische Druckunterschied zwischen einem Minimalwert ΔC_{pm} des reduzierten statischen Druckunterschied ΔC_p und einem Wert $\Delta C_{pm-0,4}$ des reduzierten statischen Druckunterschieds ΔC_p an dem Ort entsprechend dem dimensionslosen Meridionalabstand $m_{m-0,4}$ erhalten durch die Subtraktion eines dimensionslosen Meridionalabstandes 0,4 vom dimensionslosen Meridionalabstand m_m , der den Minimalwert ΔC_{pm} repräsentiert, ausgewählt ist zu:

nicht weniger als 0,20 bei der spezifischen Geschwindigkeit N_s von nicht mehr als 280,
 nicht weniger als 0,28 bei der spezifischen Geschwindigkeit von nicht mehr als 400, und
 nicht weniger als 0,35 bei der spezifischen Geschwindigkeit von nicht mehr als 560; und

wobei die deutlich abnehmende Tendenz von ΔM für die Turbomaschine, die ein verdichtbares Strömungsmittel handhabt, derart ausgelegt ist, dass der relative Machzahlunterschied zwischen einem Minimalwert ΔM_m des relativen Machzahlunterschieds ΔM und einem Wert $\Delta M_{m-0,4}$ des relativen Machzahlunterschieds ΔM an dem Ort, der dem dimensionslosen Meridionalabstand $M_{m-0,4}$ entspricht, der erhalten wird durch Subtraktion eines dimensionslosen Meridionalabstandes 0,4 vom dimensionslosen Meridionalabstand M_m , der den Minimalwert ΔM_m repräsentiert, ausgewählt ist auf nicht weniger als 0,23 bei der spezifischen Geschwindigkeit von nicht mehr als 488.

7. Verfahren zur Herstellung einer Turbomaschine nach Anspruch 6, wobei beurteilt wird ob der dimensionslose Meridionalabstand m_m , der den Minimalwert ΔC_{pm} des reduzierten statischen Druckunterschiedes ΔC_p repräsentiert, in einem Bereich von einem dimensionslosen Meridionalabstand $m=0,8-1$ liegt oder nicht.
8. Verfahren zur Herstellung einer Turbomaschine nach Anspruch 6 oder nach Anspruch 7, wobei beurteilt wird ob eine Druckunterschiedsteigung an der Seite der Umhüllung CPS-s auf der Saugoberfläche der Schaufel nicht kleiner ist als -1,3 als eine untere Grenze der Druckunterschiedsteigung an der Seite der Umhüllung CPS-s_{LIM}.
9. Verfahren zur Herstellung einer Turbomaschine nach Anspruch 6, wobei beurteilt wird ob eine Machzahlsteigung an der Seite der Umhüllung MS-s auf der Saugoberfläche der Schaufel nicht kleiner ist als -0,8 als eine untere Grenze der Machzahlsteigung an der Seite der Umhüllung MS-s_{LIM}.
10. Verfahren zur Herstellung einer Turbomaschine nach Anspruch 6 oder nach Anspruch 9, wobei beurteilt wird ob der dimensionslose Meridionalabstand m_m , der den Minimalwert ΔM_m des relativen Machzahlunterschieds ΔM

représenté, in einem Bereich des dimensionslosen Meridionalabstandes $m=0,8-1,0$ liegt.

Revendications

5

1. Turbomachine possédant une roue ayant plusieurs ailettes supportées par un moyeu sur lequel les ailettes sont espacées circonférentiellement et recouvertes d'une surface de carénage qui forme une limite externe à l'écoulement de fluide formé dans un passage d'écoulement délimitant une direction d'écoulement entre deux ailettes adjacentes, **caractérisée en ce que** :

10

la roue a une configuration telle qu'une différence réduite de pression statique ΔC_p ou une différence relative de nombre de Mach ΔM entre le moyeu et le carénage à la surface d'aspiration de l'ailette présente une tendance qui diminue remarquablement le long de l'emplacement d'une distance méridionale sans dimension m vers la sortie de la roue et est sélectionnée afin qu'elle soit inférieure à une valeur spécifiée qui dépend de la vitesse spécifique N_s de la turbomachine, la vitesse spécifique N_s étant définie par la relation $N_s = NQ^{0.5}/H^{0.75}$, N étant la vitesse de rotation en tours par minute, Q le débit à une entrée de la roue, en mètres cubes par minute, et H la hauteur en mètres représentant l'énergie du fluide qui est donnée au fluide par la turbomachine,

15

la tendance qui diminue remarquablement de ΔC_p de la turbomachine qui transmet un fluide incompressible est telle que la différence réduite de pression statique entre une valeur minimale ΔC_{pm} de la différence réduite de pression statique ΔC_p et une valeur $\Delta C_{pm-0,4}$ de la différence réduite de pression statique ΔC_p à un emplacement correspondant à la distance méridionale sans dimension $m_{m-0,4}$, obtenue par soustraction d'une distance méridionale sans dimension 0,4 de la distance méridionale sans dimension m_m qui représente la valeur minimale ΔC_{pm} est sélectionnée afin que

20

elle ne soit pas inférieure à 0,20 à la vitesse spécifique N_s qui ne dépasse pas 280,
 elle ne soit pas inférieure à 0,28 à la vitesse spécifique N_s qui ne dépasse pas 400, et
 elle ne soit pas inférieure à 0,35 à la vitesse spécifique N_s qui ne dépasse pas 560, et

25

la tendance qui diminue remarquablement de ΔM pour la turbomachine qui transmet un fluide compressible est telle que la différence relative de nombre de Mach entre la valeur minimale ΔM_m de la différence relative de nombre de Mach ΔM et une valeur $\Delta M_{m-0,4}$ de la différence relative de nombre de Mach ΔM à l'emplacement correspondant à la distance méridionale sans dimension $M_{m-0,4}$ obtenue par soustraction d'une distance méridionale sans dimension 0,4 de la distance méridionale sans dimension M_2 représentant la valeur minimale ΔM_m est sélectionnée afin qu'elle ne soit pas inférieure à 0,23 à la vitesse spécifique qui ne dépasse pas 488.

30

2. Turbomachine selon la revendication 1, dans laquelle la distance méridionale sans dimension M_m représentant la valeur minimale ΔC_{pm} de la différence réduite de pression statique ΔC_p est sélectionnée afin qu'elle soit comprise dans la plage de distance méridionale sans dimension $m = 0$ à 8,0.

35

3. Turbomachine selon la revendication 1 ou 2, dans laquelle la pente du coefficient de pression du côté du carénage CPS-s à la surface d'aspiration de l'ailette est sélectionnée afin qu'elle ne soit pas inférieure à -1,3 à une limite inférieure de la pente du coefficient de pression du côté du carénage CPS-s_{LIM}.

40

4. Turbomachine selon la revendication 1, dans laquelle la pente du nombre de Mach du côté du carénage MS-s du côté d'aspiration de l'ailette est sélectionnée afin qu'elle ne soit pas inférieure à -0,8 formant la limite inférieure de la pente du nombre de Mach du côté du carénage Ms-s_{LIM}.

45

5. Turbomachine selon la revendication 1 ou 4, dans laquelle la distance méridionale sans dimension M_2 représentant la valeur minimale ΔM de la différence relative de nombre de Mach ΔM est sélectionnée afin qu'elle soit comprise dans la plage de distance méridionale sans dimension $m = 0,8$ à 1,0.

50

6. Procédé de fabrication d'une turbomachine possédant une roue ayant plusieurs ailettes supportées par un moyeu sur lequel les ailettes sont espacées circonférentiellement et recouvertes d'une surface de carénage qui forme une limite extérieure pour l'écoulement d'un fluide dans un passage d'écoulement délimitant une direction d'écoulement entre deux ailettes adjacentes, comprenant :

55

une première étape de sélection d'une géométrie méridionale et du nombre d'ailettes de la roue à l'aide de spécifications de conception telles que des données d'entrée, délimitant plusieurs surfaces de révolution dans un canal d'écoulement méridional, et la détermination d'une condition d'empilement f_0 ,

une seconde étape de détermination d'une distribution de charge d'ailette rV_θ suivant une distance méridionale sans dimension m par sélection d'une forme de la distribution de charge d'ailette $\delta(rV_\theta)/\delta m$ qui a un pic à la surface de carénage dans la première moitié de l'emplacement de la distance non méridionale m et un pic à la surface de moyeu dans la dernière moitié de l'emplacement de la distance méridionale sans dimension, et d'ajustement d'une valeur obtenue par intégration de la distribution de charge d'ailette le long de la distance méridionale sans dimension m afin que la hauteur nominale de la roue soit obtenue, une troisième étape de détermination d'une géométrie tridimensionnelle de la roue par intégration de

$$\{(\bar{V}_z + v_{zb1})\delta f/\delta z\} + \{(\bar{V}_r + v_{rb1})\delta f/\delta r\} = \{(r\bar{V}_\theta)/r^2\} + \{(v_{ob1})/r\} - \omega$$

le long de la distance méridionale sans dimension m avec la condition d'empilement f_0 comme valeur initiale pour la détermination de la coordonnée tangentielle f de la ligne de cambrure d'ailette à une distance méridionale sans dimension m , et d'addition d'une certaine épaisseur à la valeur déterminée pour que l'ailette puisse avoir la résistance mécanique nécessaire,

une quatrième étape de détermination du fait que l'une des distributions de différence réduite de pression statique ΔC_p et de distribution de différence relative de nombre de Mach ΔM le long de la distance méridionale sans dimension m obtenue dans la troisième étape convient ou non à la suppression de l'écoulement secondaire dans la roue,

une cinquième étape d'évaluation de la possibilité de mauvaises performances dues à au moins une séparation de l'écoulement dans la roue, déterminée par la troisième étape, d'évaluation de l'écoulement secondaire dans la roue par un paramètre d'écoulement secondaire puis, après retour à la seconde étape pour la modification de la distribution de charge d'ailette d'après l'évaluation précédente, de répétition des étapes précédentes jusqu'à ce que le résultat prévu soit obtenu,

dans lequel une différence réduite de pression statique ΔC_p ou une différence relative de nombre de Mach ΔM entre le moyeu et le carénage à la surface d'aspiration de l'ailette présente une tendance qui diminue remarquablement le long de l'emplacement d'une distance méridionale sans dimension m vers la sortie de la roue et est sélectionnée afin qu'elle soit inférieure à une valeur spécifiée qui dépend de la vitesse spécifique N_s de la turbomachine, la vitesse spécifique N_s étant définie par la relation $N_s = NQ^{0.5}/H^{0.75}$, N étant la vitesse de rotation en tours par minute, Q le débit à une entrée de la roue, en mètres cubes par minute, et H la hauteur en mètres représentant l'énergie du fluide qui est donnée au fluide par la turbomachine,

la tendance qui diminue remarquablement de ΔC_p de la turbomachine qui transmet un fluide incompressible est telle que la différence réduite de pression statique entre une valeur minimale ΔC_{pm} de la différence réduite de pression statique ΔC_p et une valeur $\Delta C_{pm-0,4}$ de la différence réduite de pression statique ΔC_p à un emplacement correspondant à la distance méridionale sans dimension $m_{m-0,4}$, obtenue par soustraction d'une distance méridionale sans dimension 0,4 de la distance méridionale sans dimension m_m qui représente la valeur minimale ΔC_{pm} est sélectionnée afin que

elle ne soit pas inférieure à 0,20 à la vitesse spécifique N_s qui ne dépasse pas 280,

elle ne soit pas inférieure à 0,28 à la vitesse spécifique N_s qui ne dépasse pas 400, et

elle ne soit pas inférieure à 0,35 à la vitesse spécifique N_s qui ne dépasse pas 560, et

la tendance qui diminue remarquablement de ΔM pour la turbomachine qui transmet un fluide compressible est telle que la différence relative de nombre de Mach entre la valeur minimale ΔM_m de la différence relative de nombre de Mach ΔM et une valeur $\Delta M_{m-0,4}$ de la différence relative de nombre de Mach ΔM à l'emplacement correspondant à la distance méridionale sans dimension $M_{m-0,4}$ obtenue par soustraction d'une distance méridionale sans dimension 0,4 de la distance méridionale sans dimension M_2 représentant la valeur minimale ΔM_m est sélectionnée afin qu'elle ne soit pas inférieure à 0,23 à la vitesse spécifique qui ne dépasse pas 488.

7. Procédé de fabrication d'une turbomachine selon la revendication 6, dans lequel il est déterminé si la distance méridionale sans dimension m_m représentant la valeur minimale ΔC_{pm} de la différence réduite de pression statique ΔC_p se trouve dans la plage de distance méridionale sans dimension $m = 0,8$ à 1 ou non.

8. Procédé de fabrication d'une turbomachine selon la revendication 6 ou 7, dans lequel il est déterminé si la pente du coefficient de pression du côté du carénage CPS-s à la surface d'aspiration de l'ailette n'est pas inférieure à -1,3 formant la limite inférieure de la pente du coefficient de pression du côté du carénage CPS-s_{LIM} ou non.

9. Procédé de fabrication d'une turbomachine selon la revendication 6, dans lequel il est déterminé si la pente du nombre de Mach du côté du carénage MS-s à la surface d'aspiration de l'ailette n'est pas inférieure à -0,8 formant

EP 0 865 577 B1

la limite inférieure de la pente du nombre de Mach du côté du carénage MS-S_{LIM} ou non.

10. Procédé de fabrication d'une turbomachine selon la revendication 6 ou 9, dans lequel il est déterminé si la distance méridionale sans dimension m_m représentant la valeur minimale ΔM_m de la différence relative de nombre de Mach ΔM est comprise dans la plage de distance méridionale sans dimension $m = 0,8$ à $1,0$ ou non.

5

10

15

20

25

30

35

40

45

50

55

FIG. 1(A)

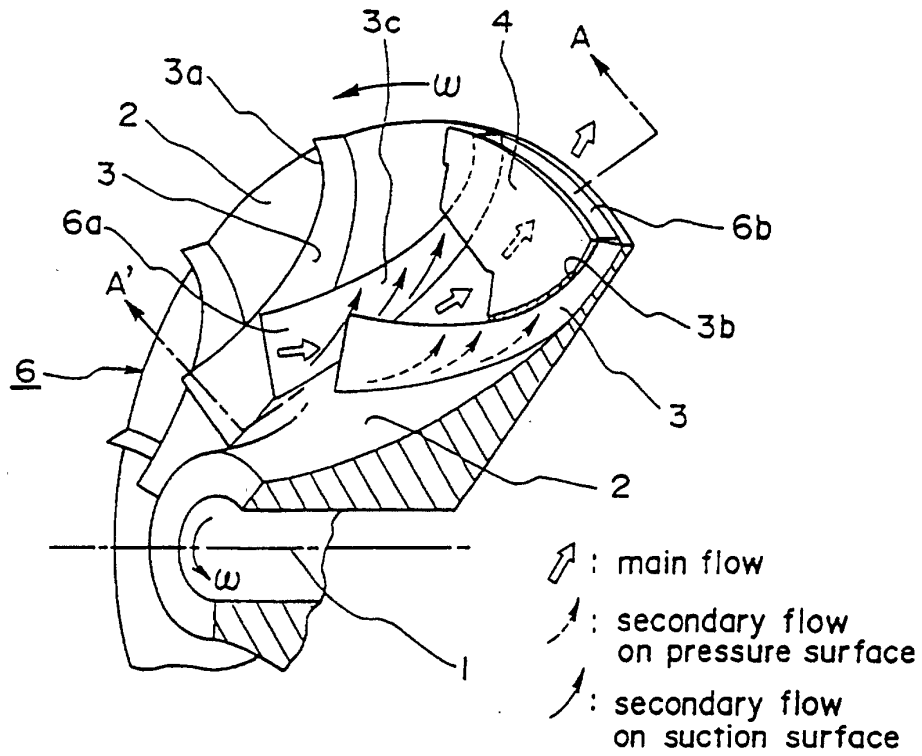


FIG. 1(B)

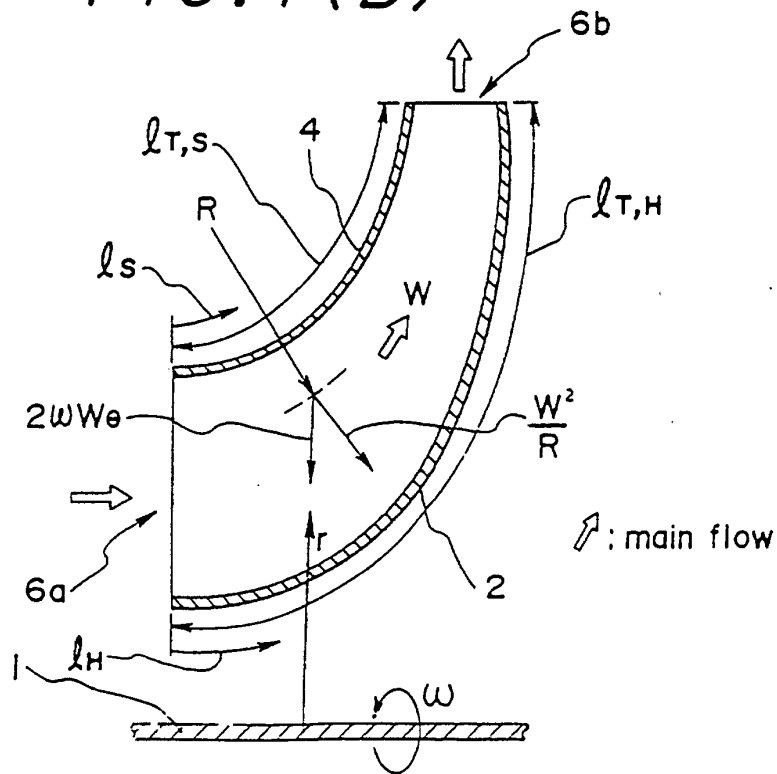


FIG. 1(C)

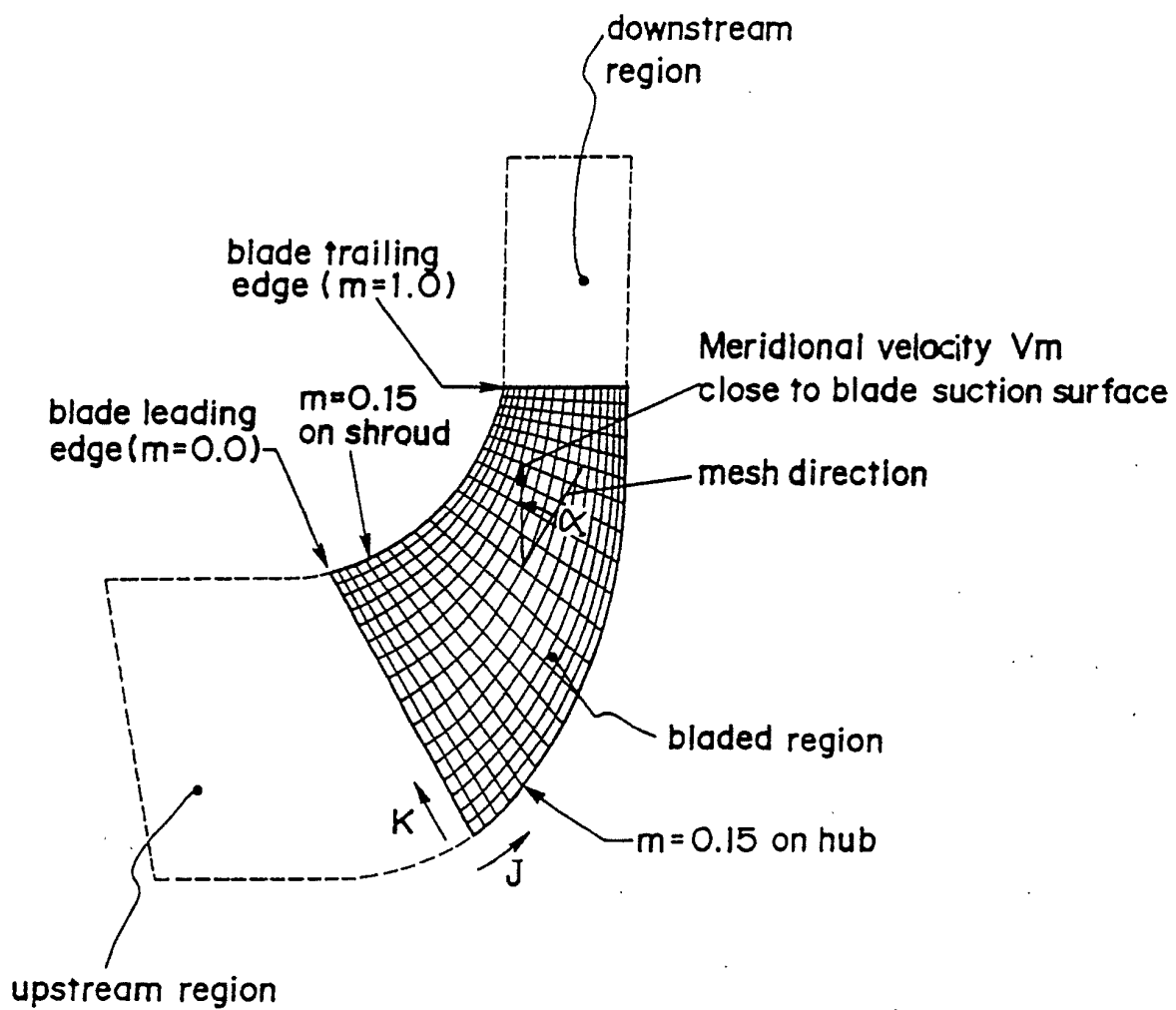


FIG. 1(D)

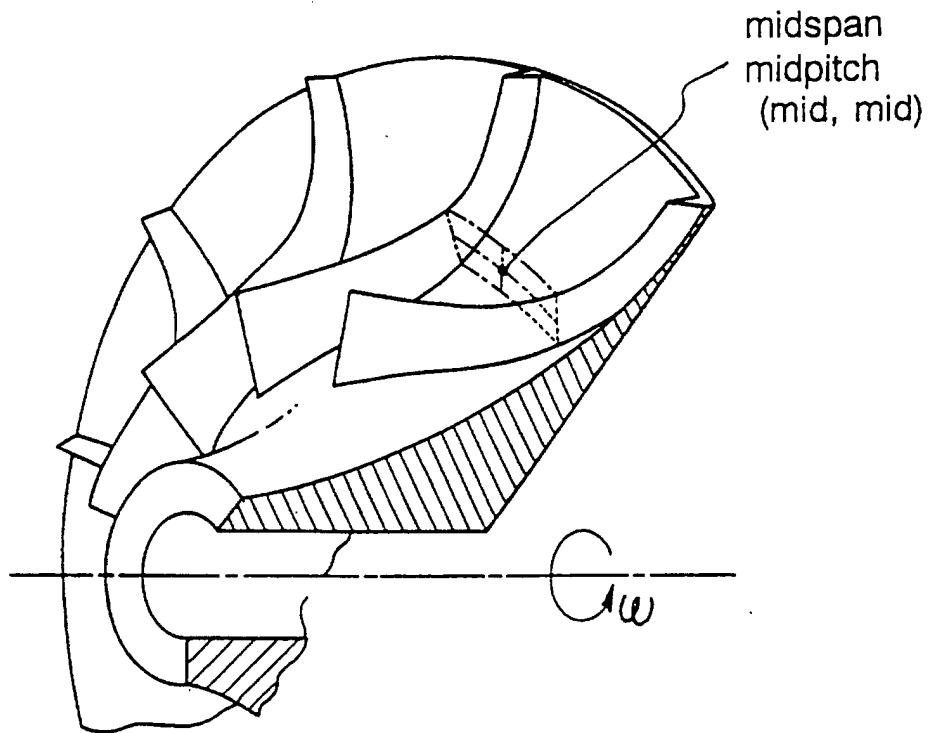


FIG. 1 (E)

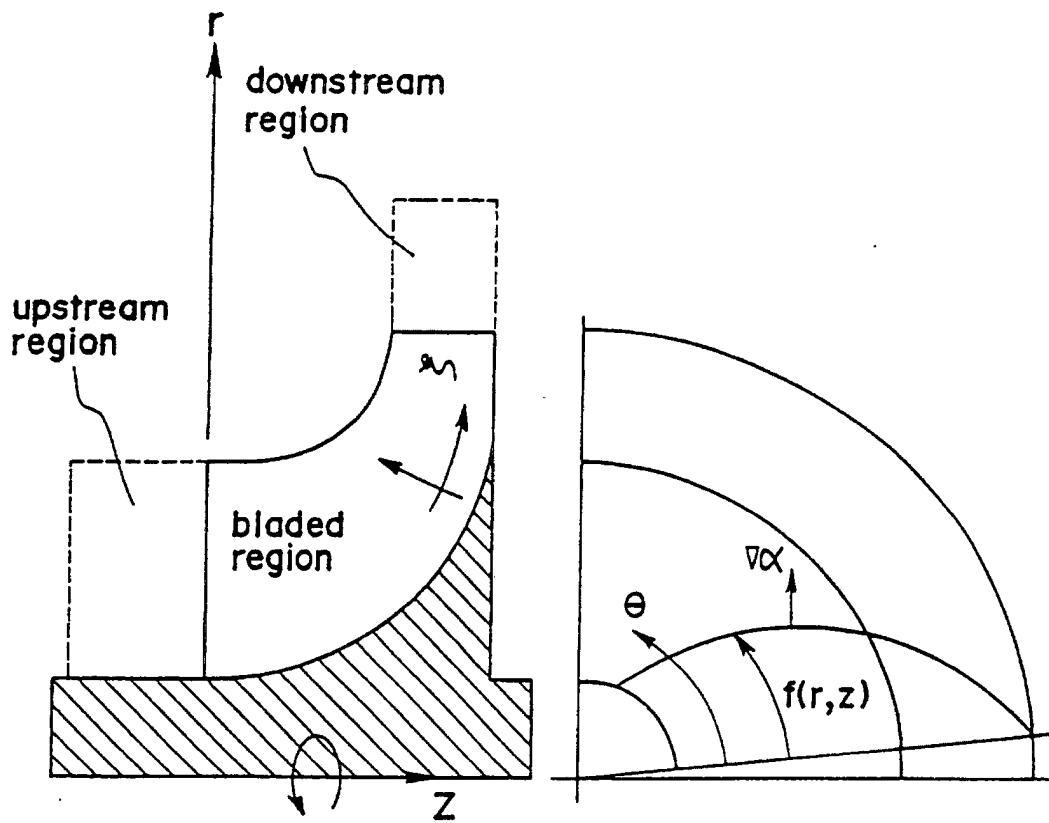


FIG. 2(A)

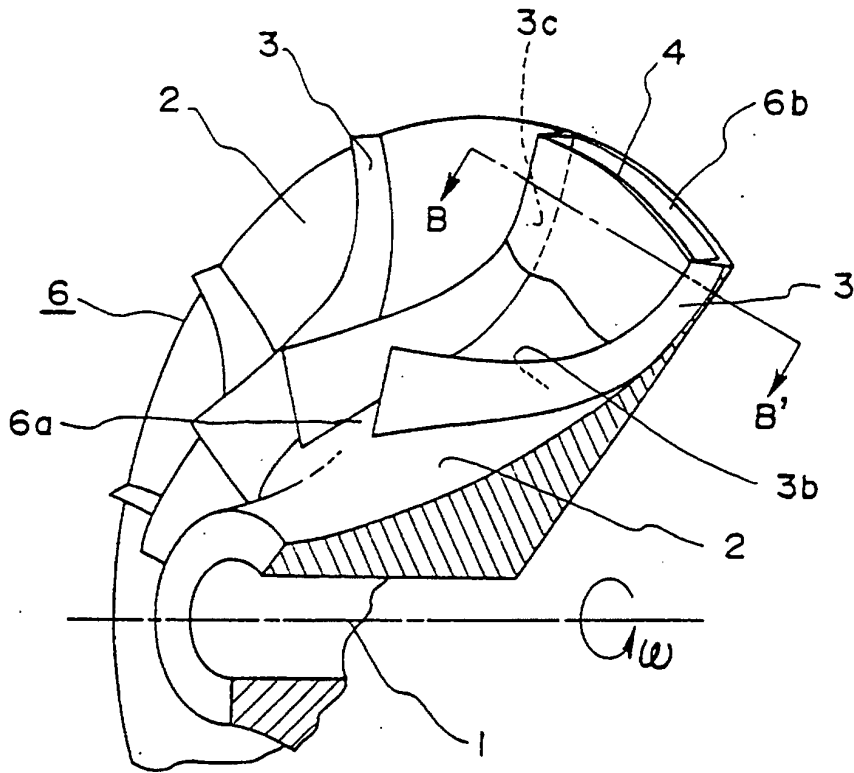


FIG. 2(B)

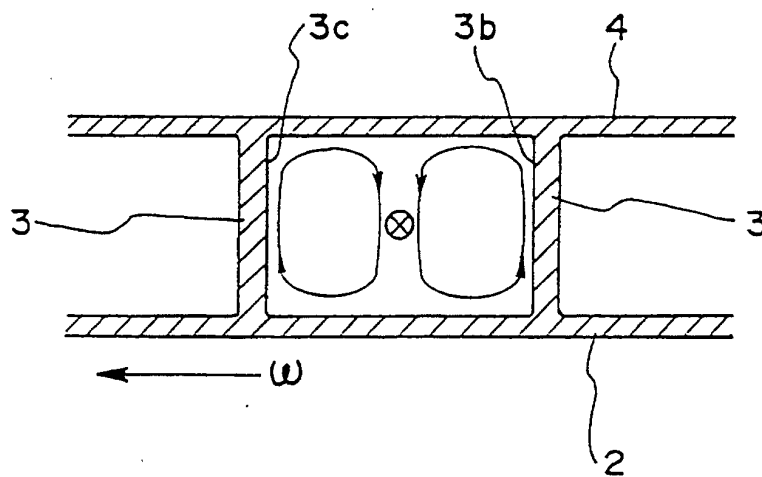


FIG. 3(A)

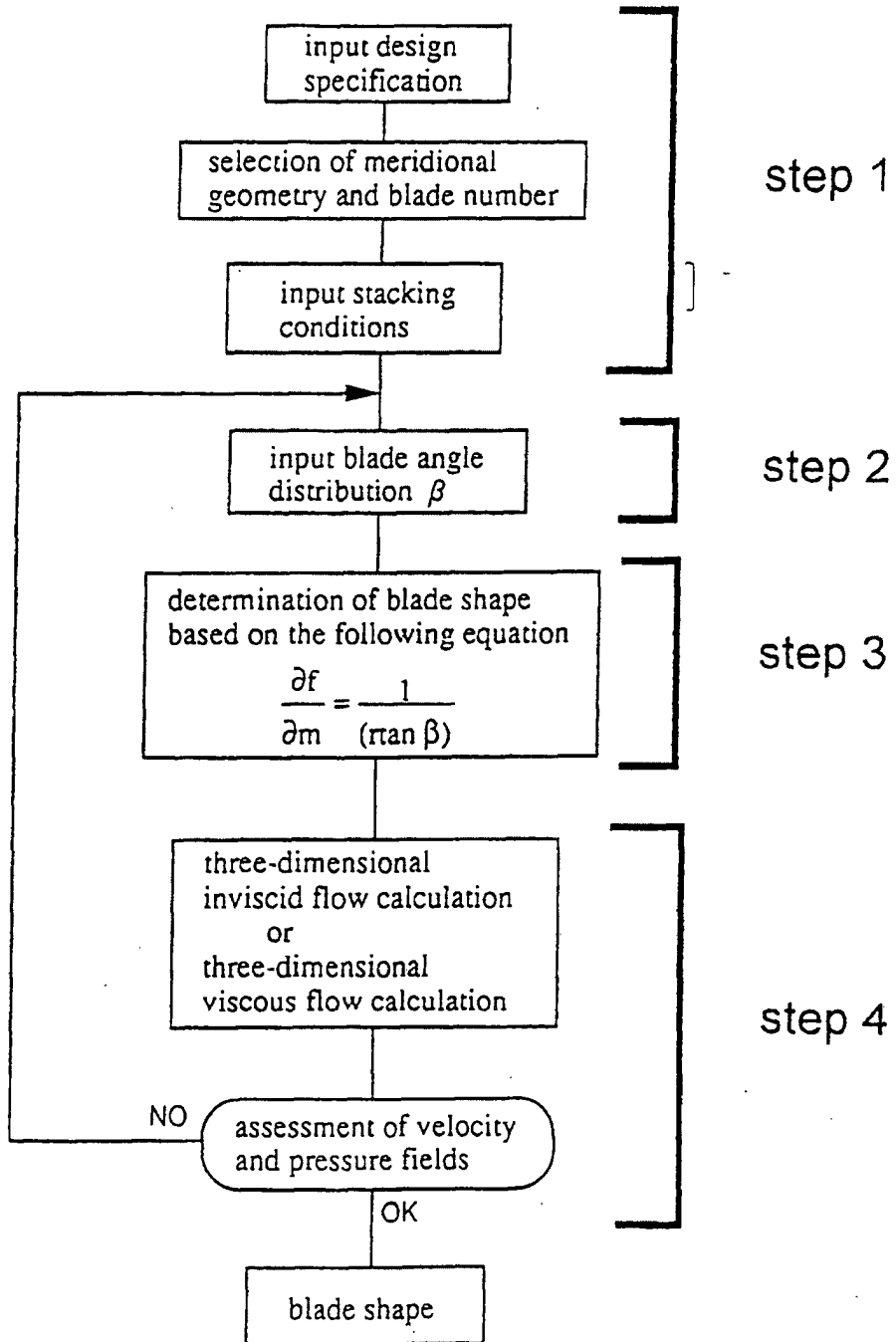


FIG. 3(B)

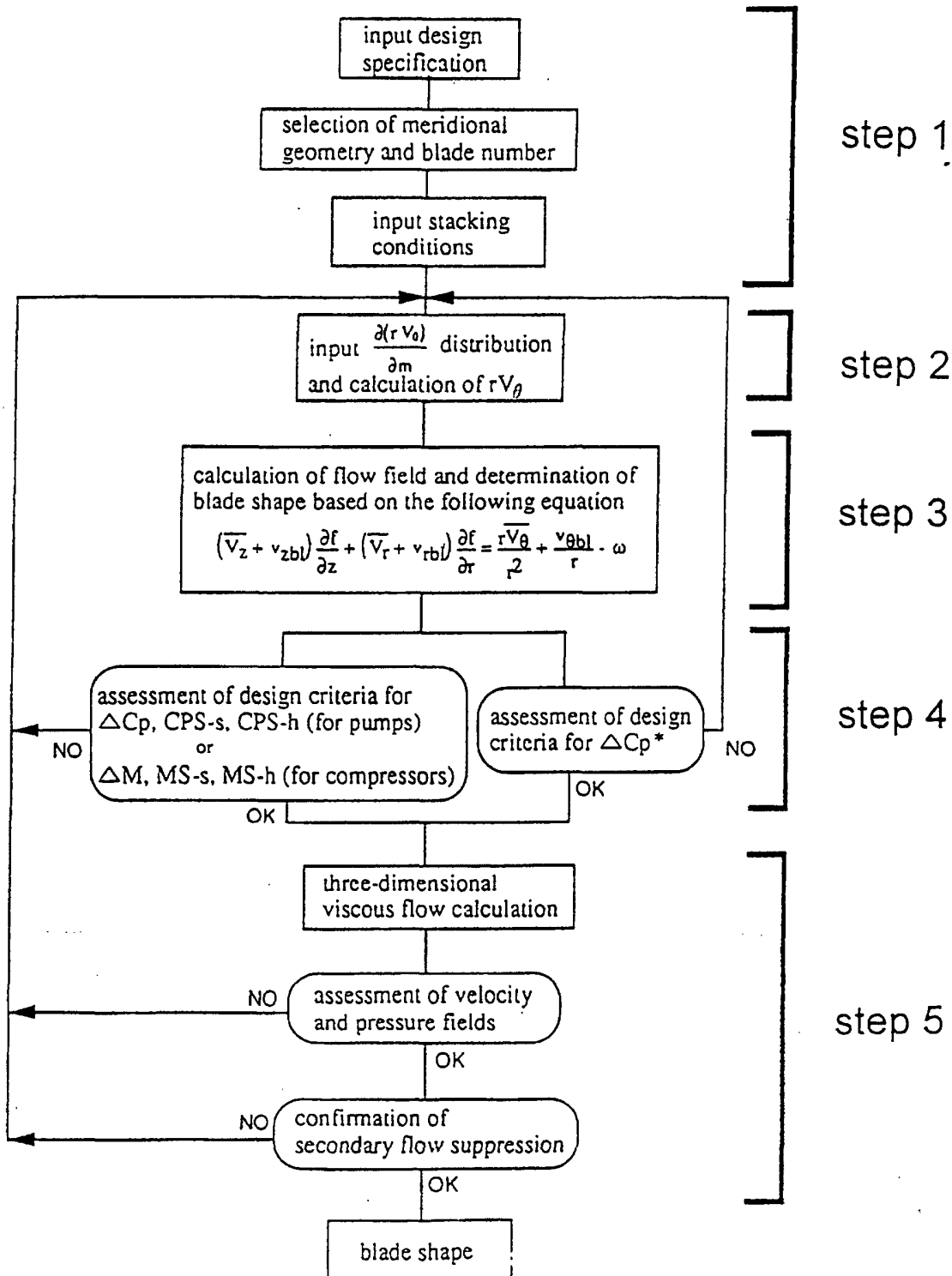


FIG. 4

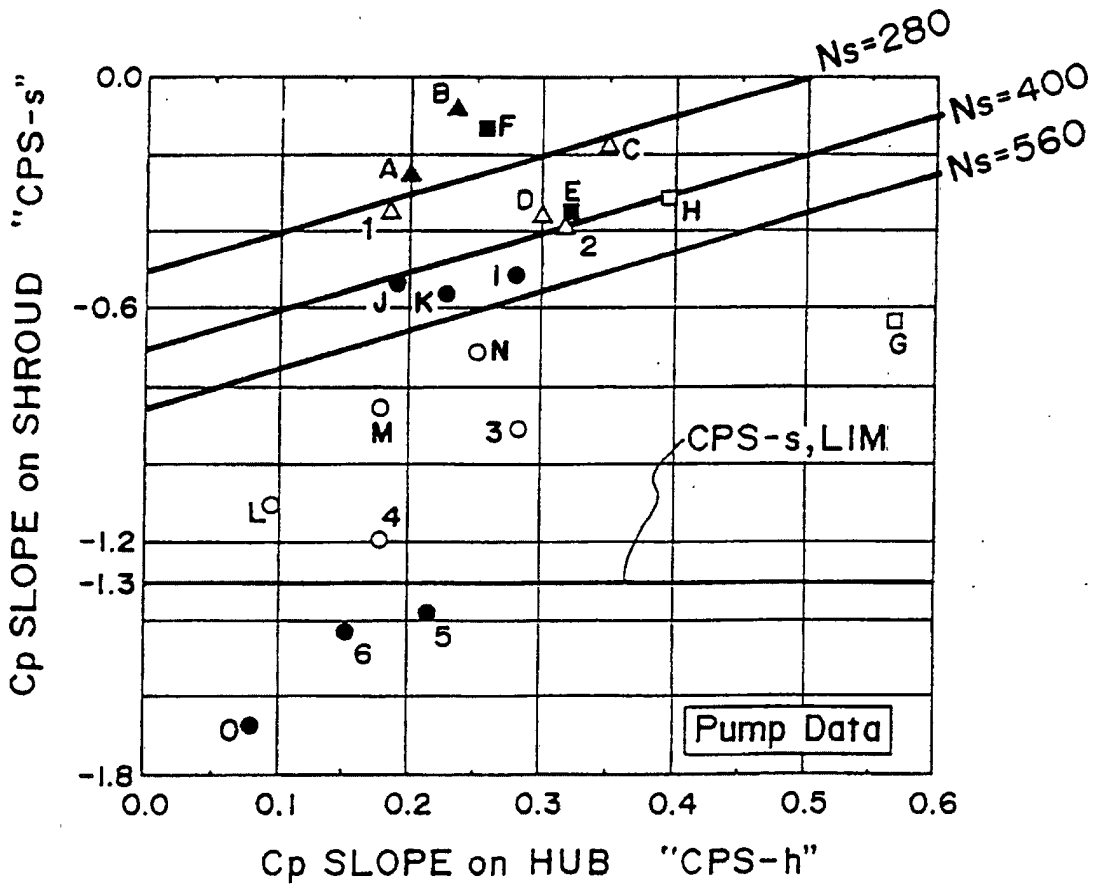


FIG. 5

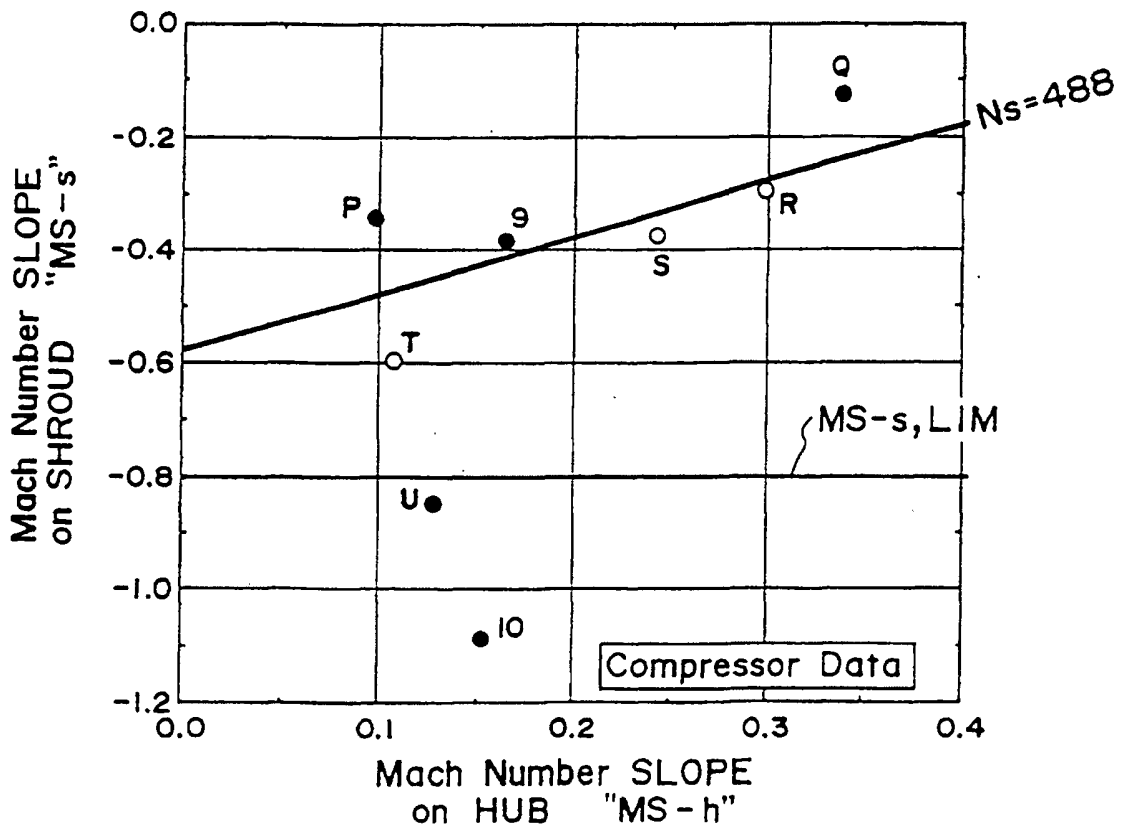


FIG. 6

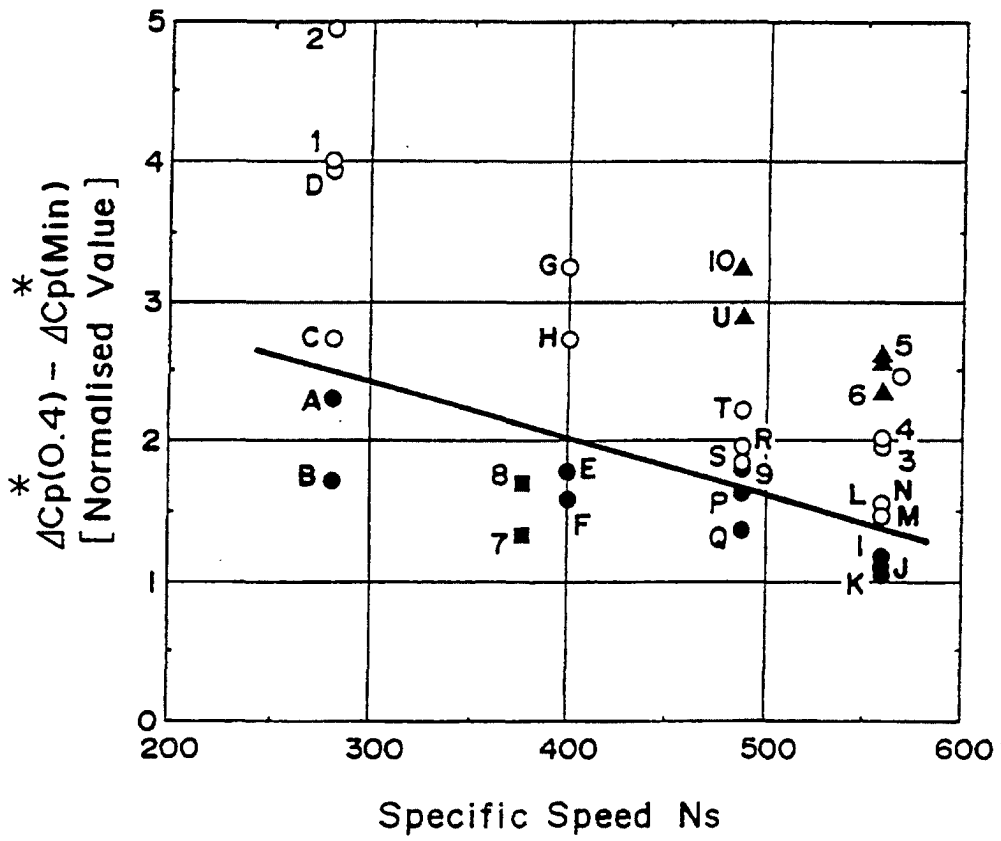


FIG. 7(A)

Machine Type	Ns	No.	CPS-h	CPS-s	MSF_angle (deg.)	
Pump	280	A	0.200	-0.250	19.9	
		B	0.235	-0.082	19.2	
		C	0.350	-0.175	17.5	
		△	D	0.300	-0.358	15.3
		1	0.185	-0.345	15.3	
		2	0.317	-0.386	15.2	
	400	□	E	0.322	-0.350	23.8
			F	0.257	-0.136	16.6
			G	0.569	-0.633	14.8
			H	0.396	-0.317	12.5
	560	○	I	0.281	-0.516	39.1
			J	0.190	-0.537	28.7
			K	0.227	-0.562	28.4
			L	0.094	-1.102	22.0
			M	0.178	-0.853	15.3
			N	0.251	-0.713	14.6
			3	0.283	-0.910	8.5
			4	0.178	-1.194	6.4
			5	0.214	-1.387	STALL
			6	0.152	-1.433	STALL
O	0.080	-1.675	STALL			

Machine Type	Ns	No.	MS-h	MS-s	MSF_angle (deg.)	
Compressor	488	P	0.098	-0.343	21.5	
		9	0.165	-0.383	20.5	
		Q	0.340	-0.125	19.1	
		R	0.300	-0.295	14.8	
		○	S	0.243	-0.375	9.5
		T	0.108	-0.595	7.1	
		U	0.128	-0.850	STALL	
		IO	0.153	-1.088	STALL	

FIG. 7(B)

Machine Type	Ns	No.	$\Delta C_p^* m - 0.4 - \Delta C_p^* m$	MSF_angle (deg.)
Pump	280	A	2.300	19.9
		B	1.720	19.2
		C	2.740	17.5
		D	3.950	15.3
		1	4.020	15.3
		2	4.950	15.2
	400	E	1.780	23.8
		F	1.580	16.6
		G	3.260	14.8
		H	2.730	12.5
	560	I	1.170	39.1
		J	1.050	28.7
		K	1.100	28.4
		L	1.550	22.0
		M	1.470	15.3
		N	1.560	14.6
		3	1.970	8.5
		4	2.020	6.4
		5	2.620	STALL
		6	2.350	STALL
377	7	1.330	STALL	
	8	1.705	STALL	

Machine Type	Ns	No.	MS-h	MSF_angle (deg.)
Compressor	488	P	1.621	21.5
		9	1.806	20.5
		Q	1.365	19.1
		R	1.954	14.8
		S	1.850	9.5
		T	2.216	7.1
	▲	U	2.900	STALL
		10	3.240	STALL

FIG. 8

(A)

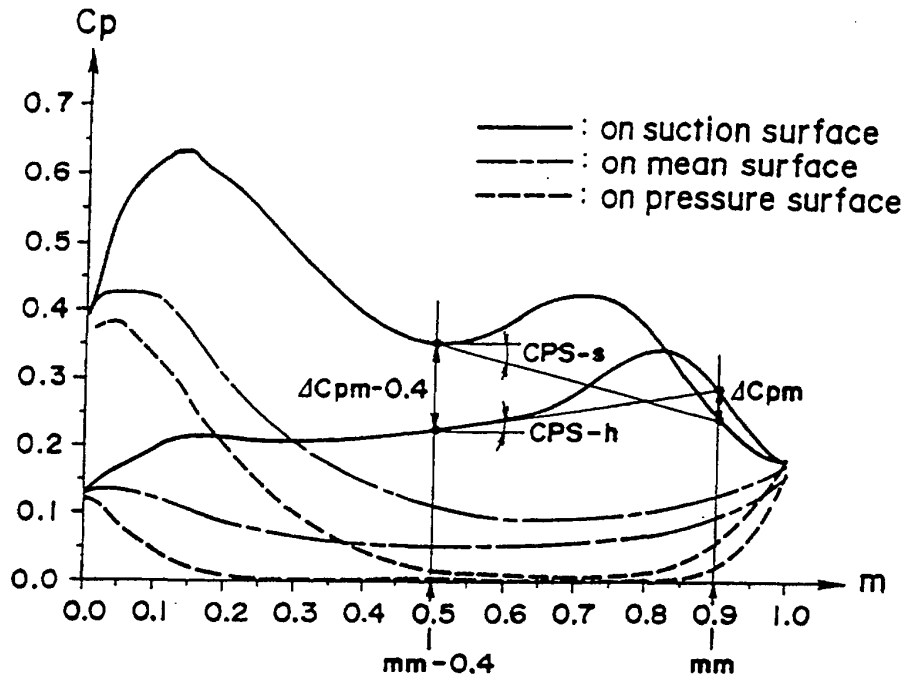


FIG. 9

(B)

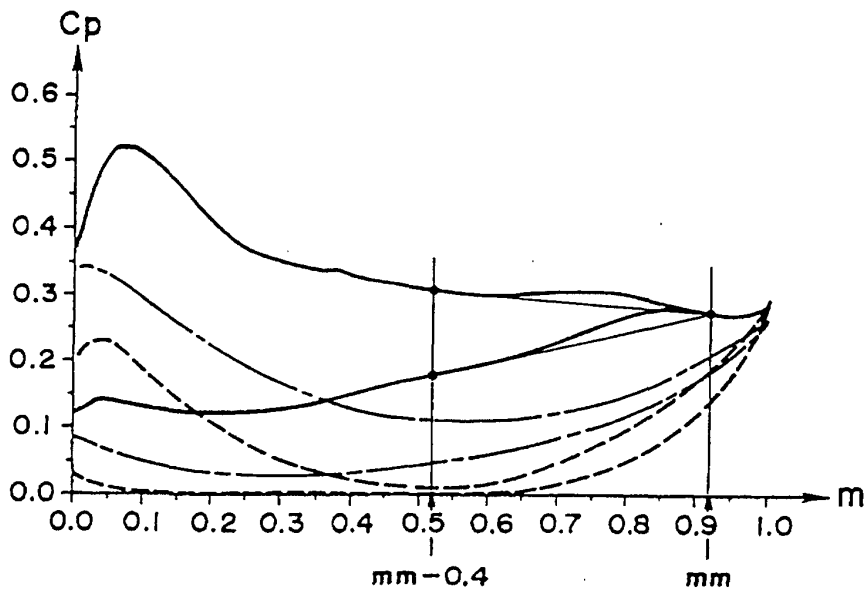


FIG. 10

(C)

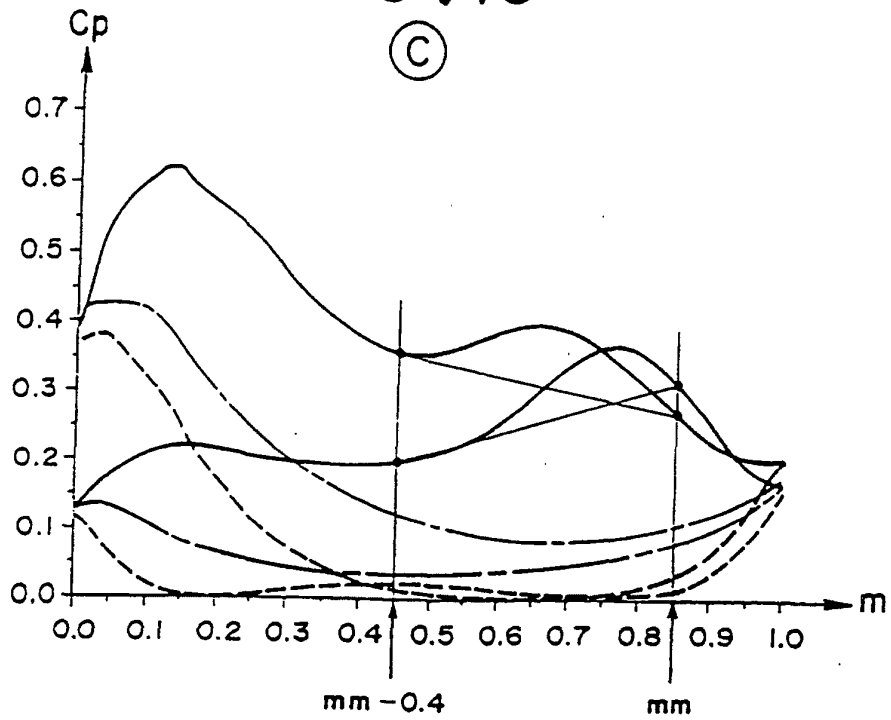


FIG. 11

(D)

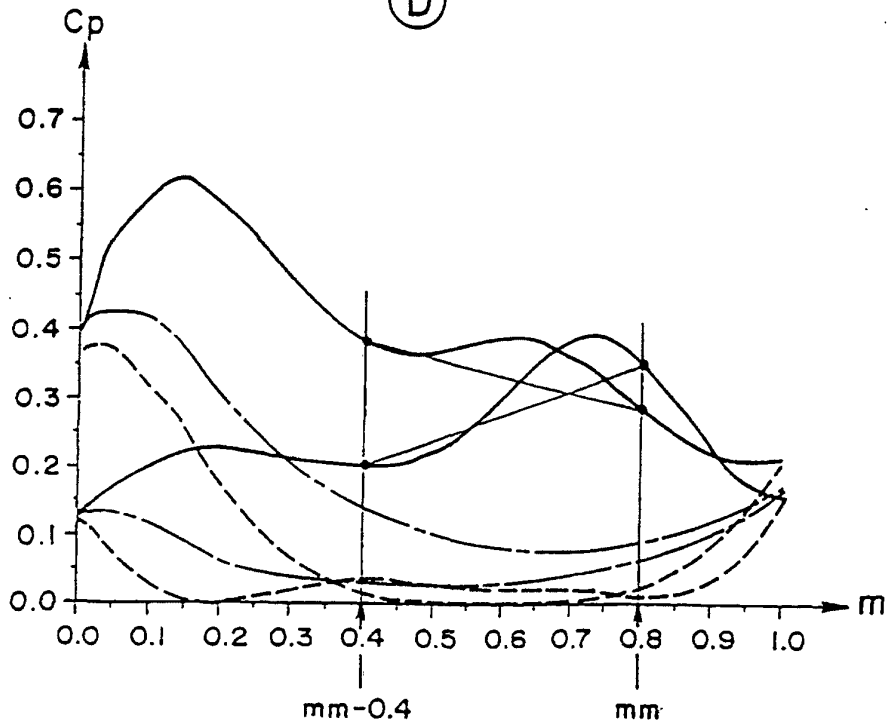


FIG. 12

(E)

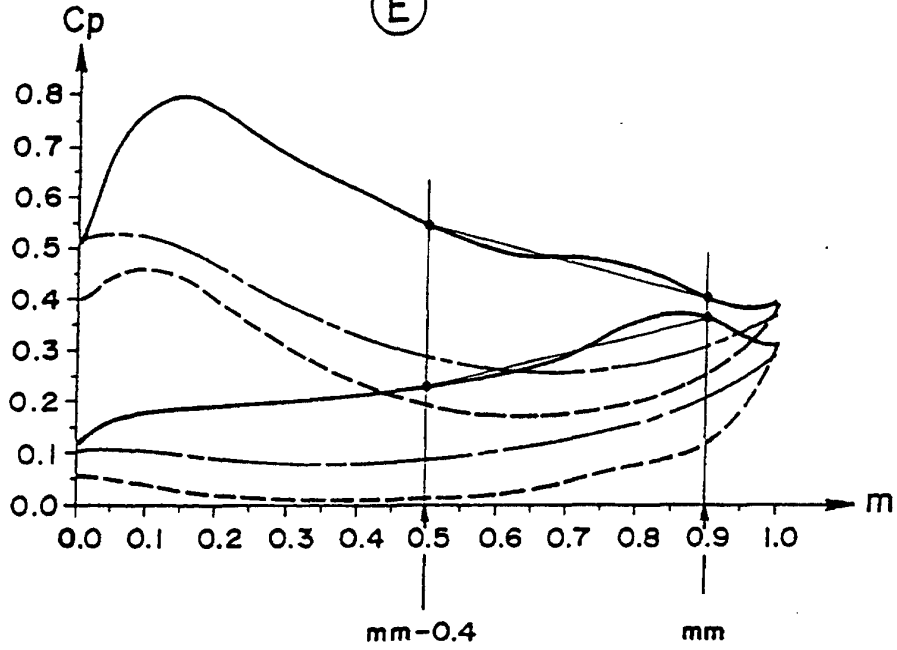


FIG. 13

(F)

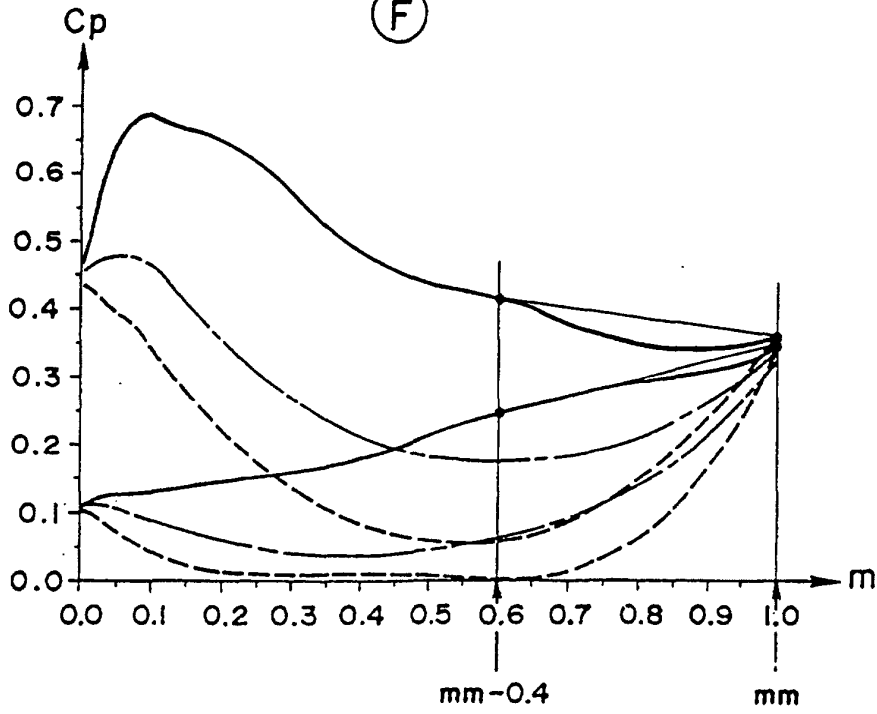


FIG. 14

(G)

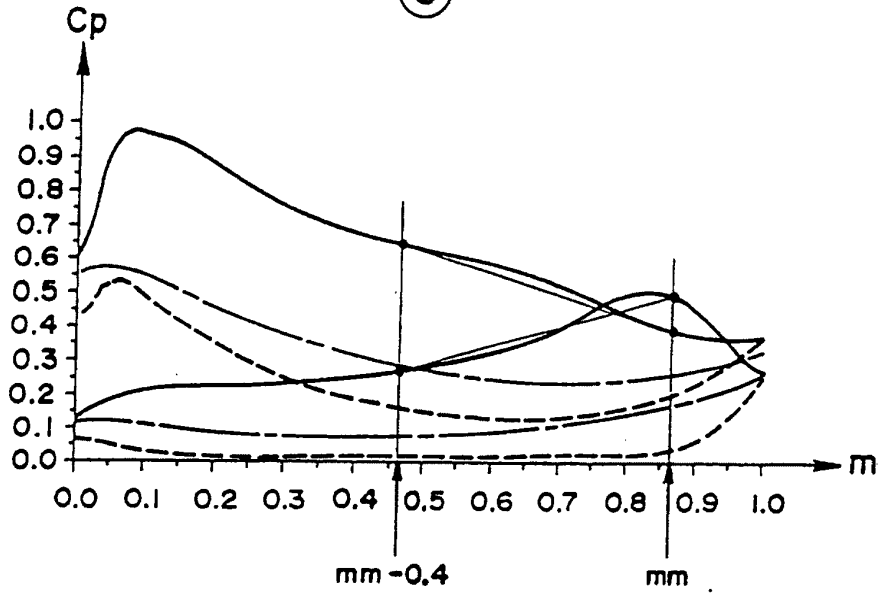


FIG. 15

(H)

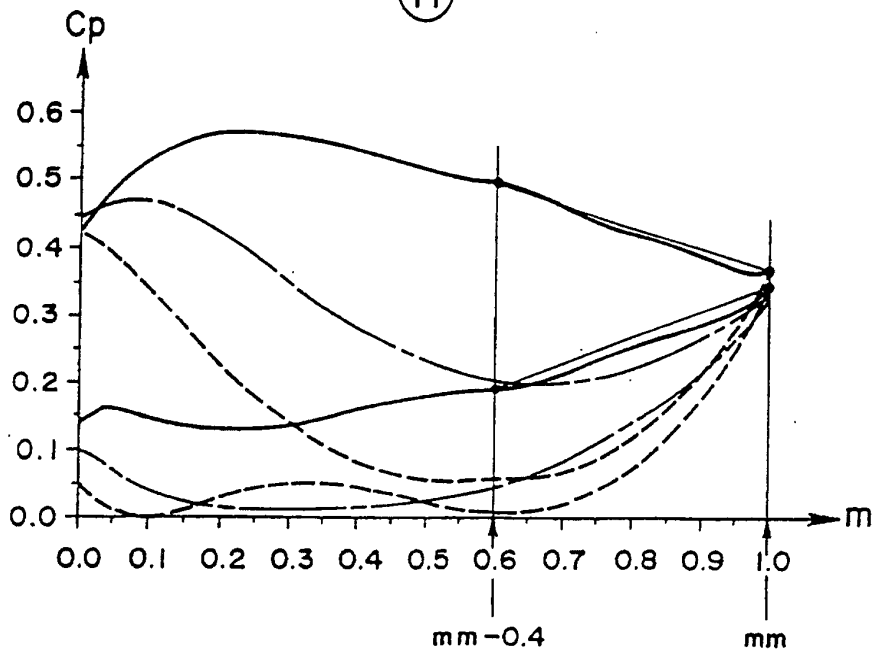


FIG. 16

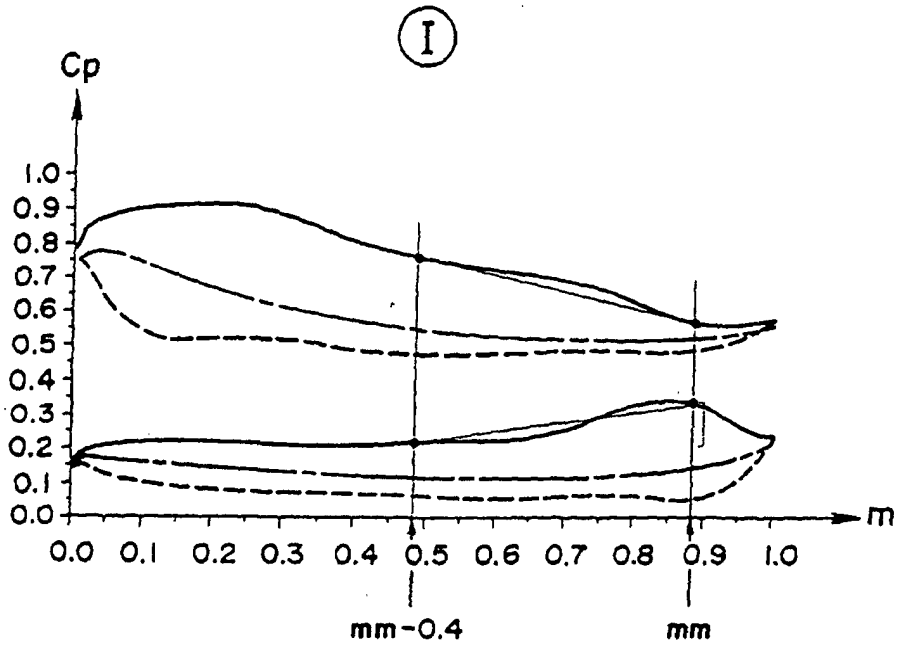


FIG. 17

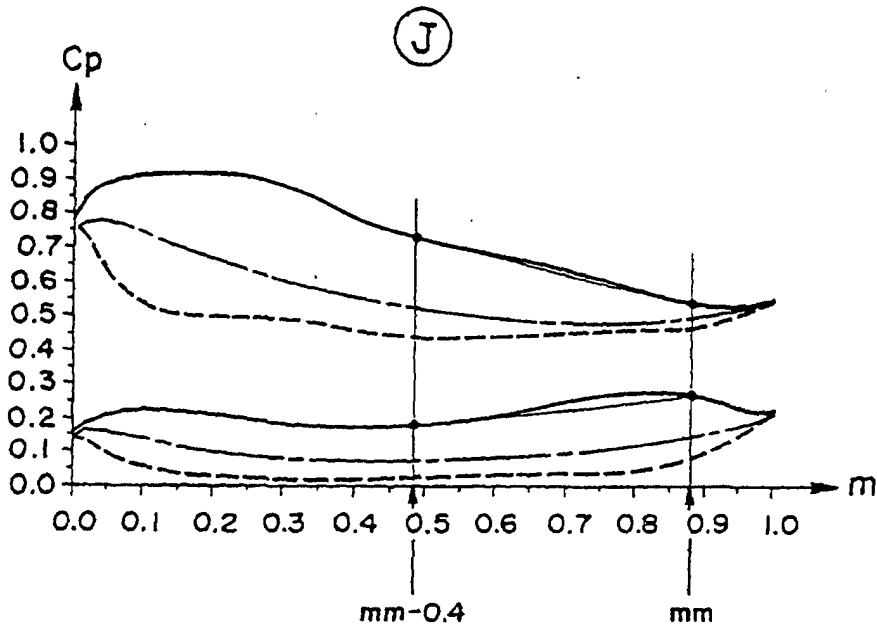


FIG. 18

(K)

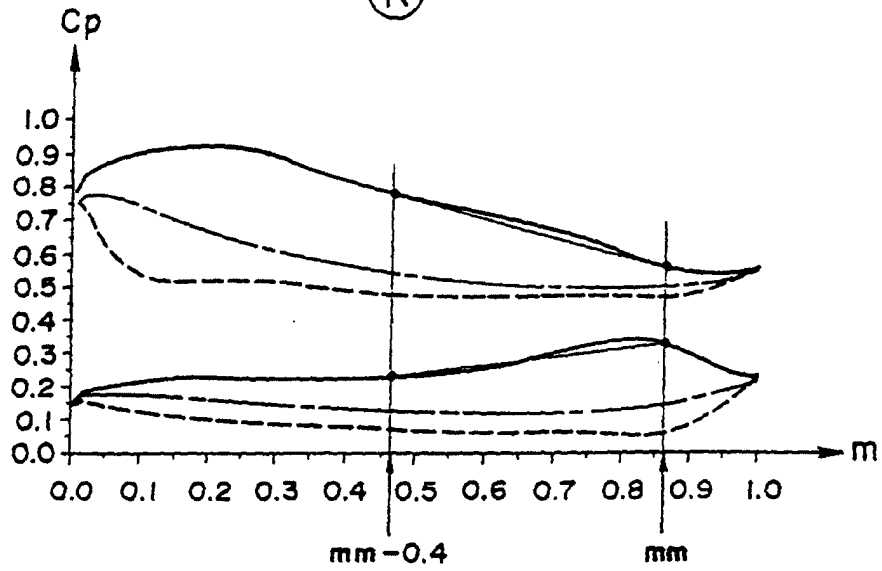


FIG. 19

(L)

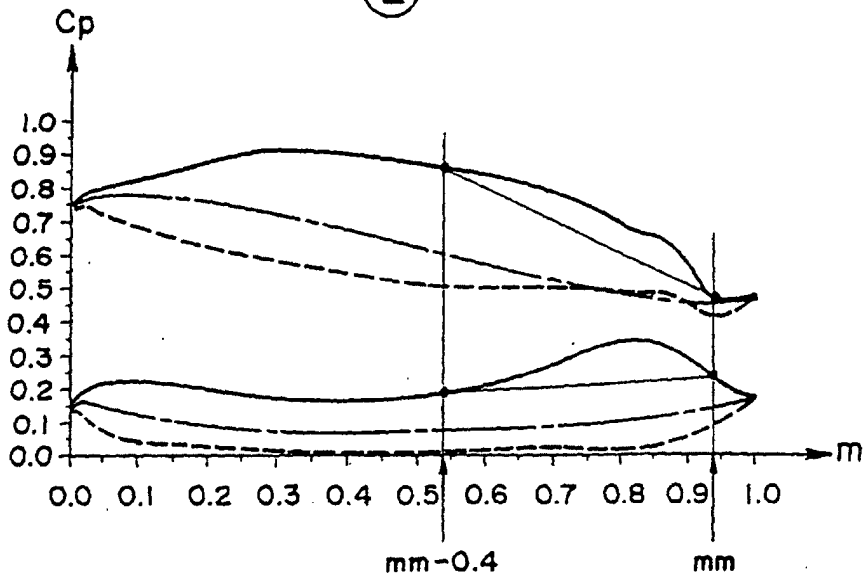


FIG. 20

(M)

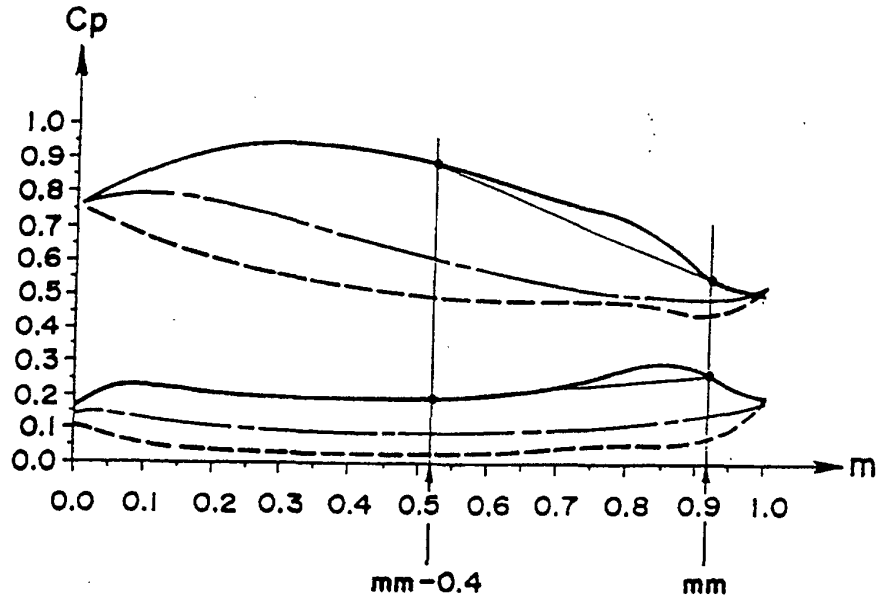


FIG. 21

(N)

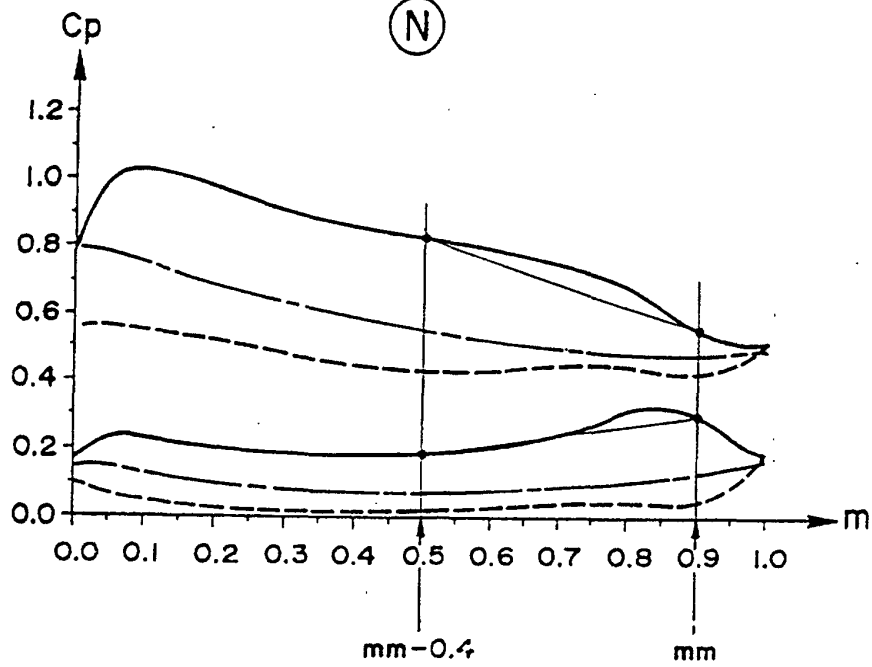


FIG. 22

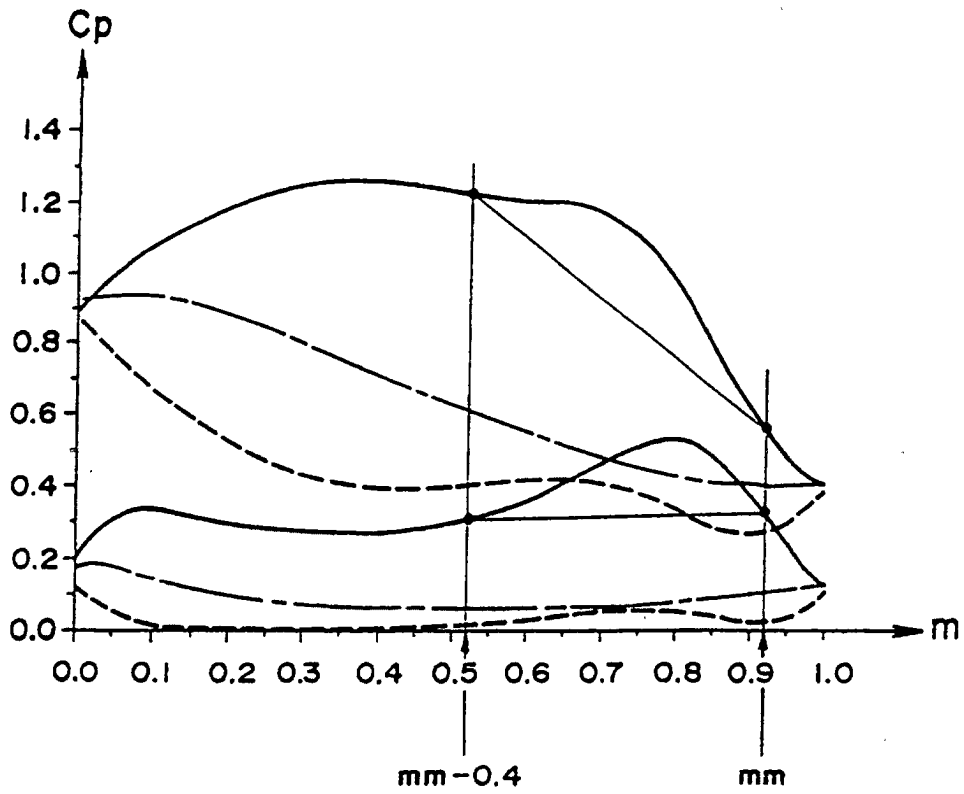


FIG. 23

①

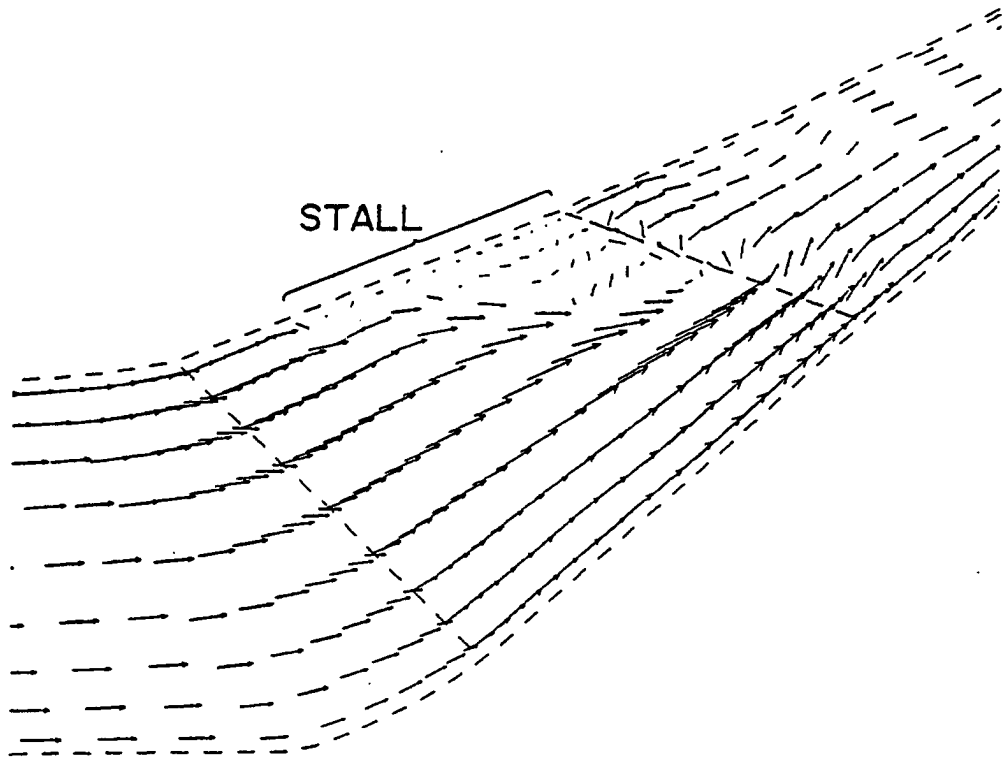


FIG. 24

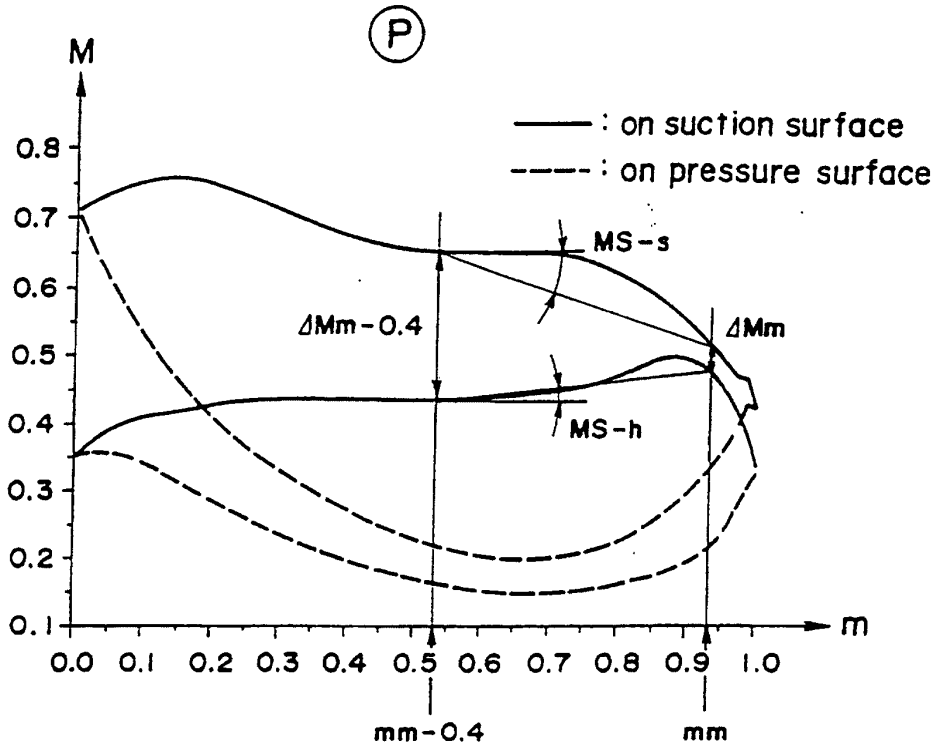


FIG. 25

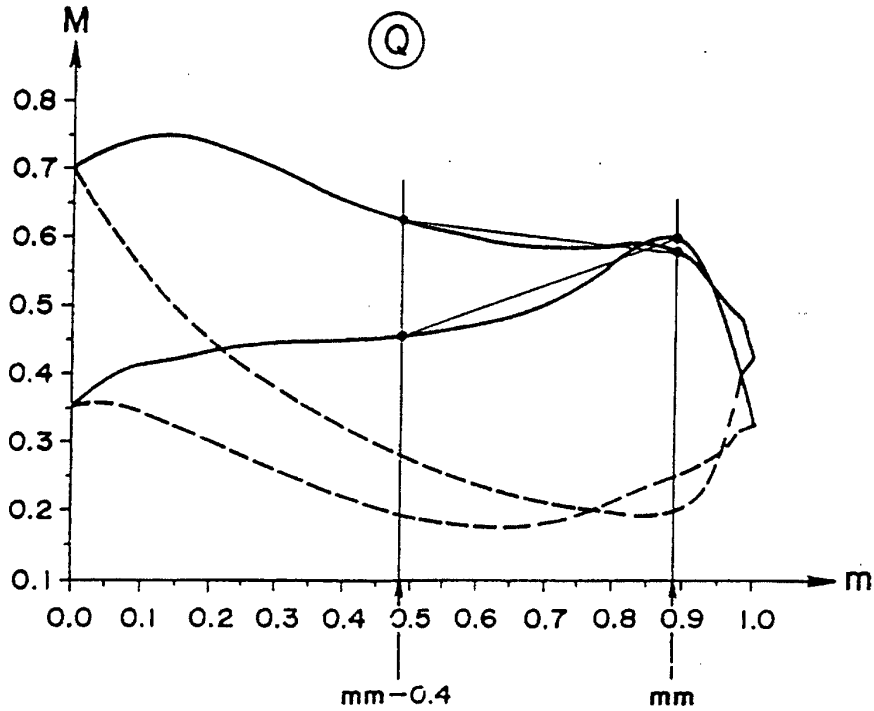


FIG. 26

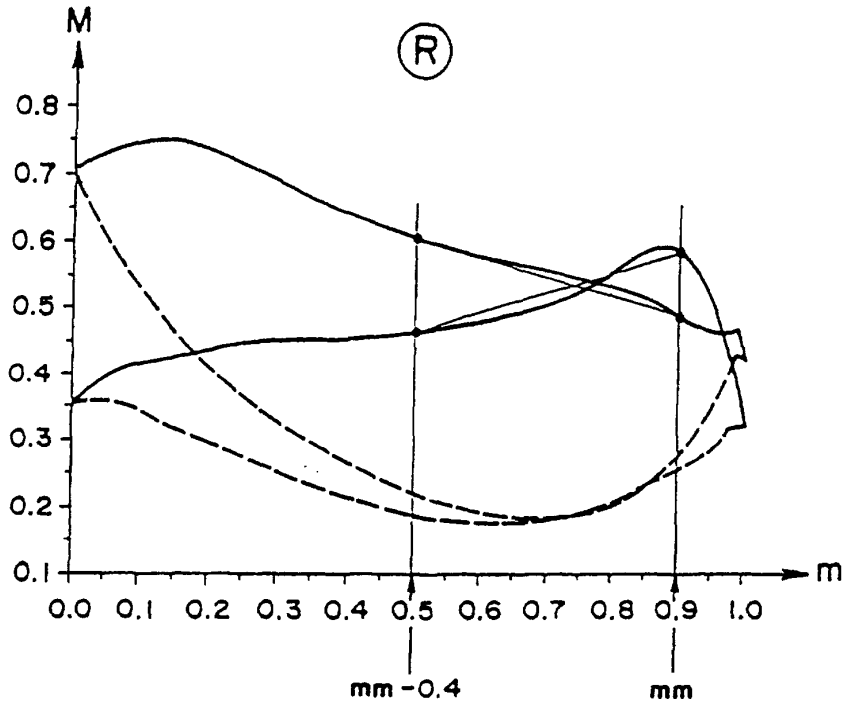


FIG. 27

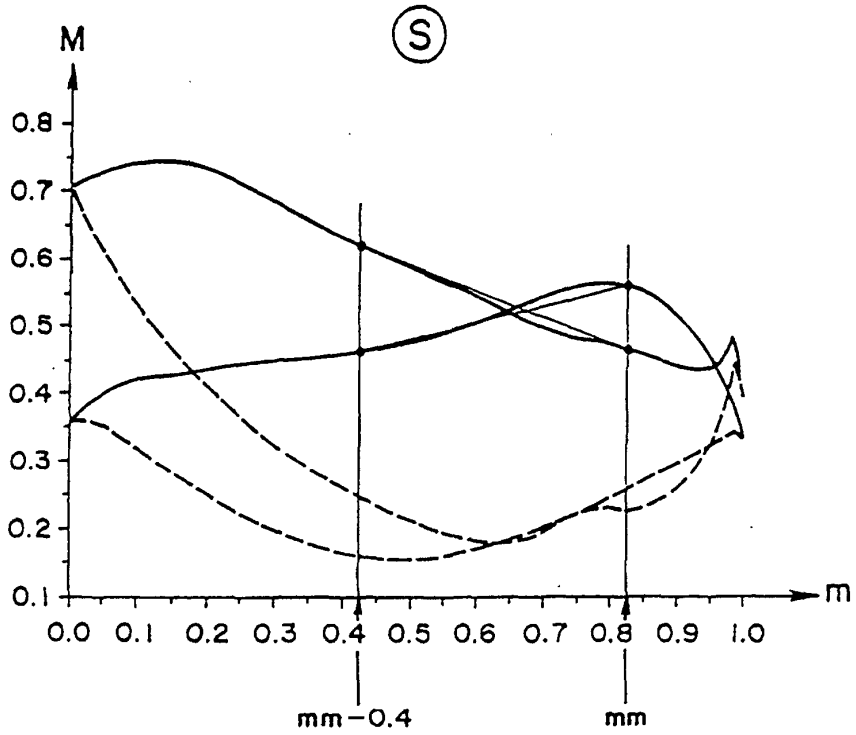


FIG. 28

(T)

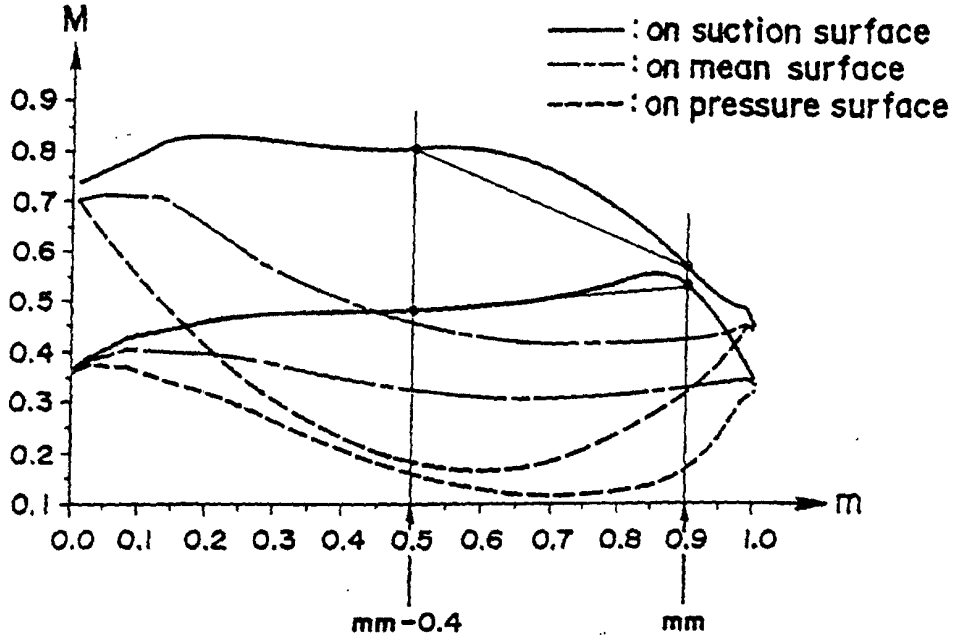


FIG. 29

(U)

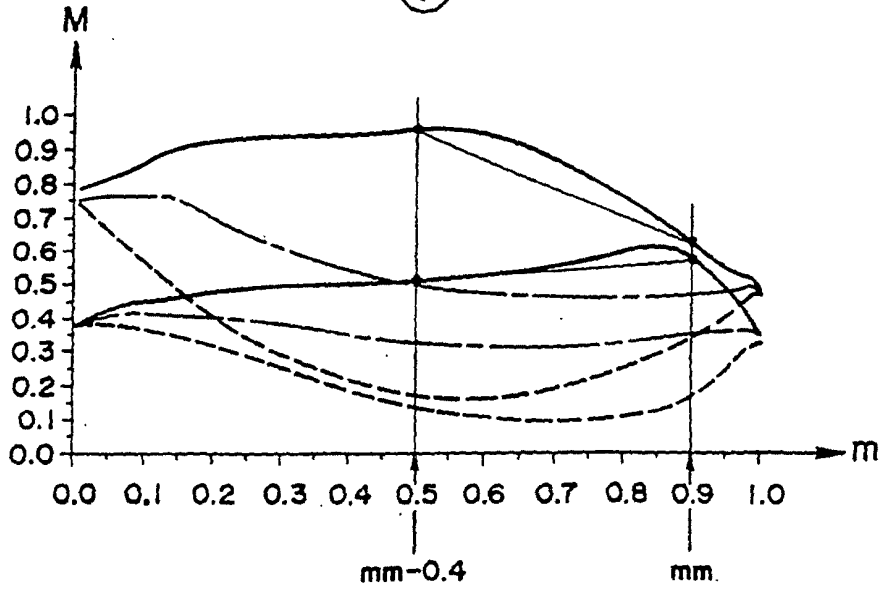


FIG. 30

U

